Copper-based composite sintering materials and reliability analysis for power electronics packaging

Wang, Xinyue; Yang, Zhoudong; Bian, Letao; Liu, Wenting; Zhang, Guoqi; Zhang, Jing; Chen, Chuantong; Liu, Pan

DOI
10.1016/j.jsamd.2025.100963

Publication date
2025

Document Version
Final published version

Published in
Journal of Science: Advanced Materials and Devices

Citation (APA)
Wang, X., Yang, Z., Bian, L., Liu, W., Zhang, G., Zhang, J., Chen, C., & Liu, P. (2025). Copper-based composite sintering materials and reliability analysis for power electronics packaging. *Journal of Science: Advanced Materials and Devices*, *10*(3), Article 100963. https://doi.org/10.1016/j.jsamd.2025.100963

Journal of Science: Advanced Materials and Devices 10 (2025) 100963

Contents lists available at ScienceDirect

Journal of Science: Advanced Materials and Devices

journal homepage: www.elsevier.com/locate/jsamd

Review Article

Copper-based composite sintering materials and reliability analysis for power electronics packaging

Xinyue Wang [a], Zhoudong Yang [a], Letao Bian [a], Wenting Liu [a], Guoqi Zhang [b], Jing Zhang [c], Chuantong Chen [d], Pan Liu [a,e,*]

[a] College of Intelligent Robotics and Advanced Manufacturing, Fudan University, Shanghai, China
[b] Department of Microelectronics, Delft University of Technology, Delft, the Netherlands
[c] Heraeus Materials Technology Shanghai Ltd., Shanghai, China
[d] Flexible 3D System Integration Laboratory, SANKEN, Osaka University, Osaka, Japan
[e] Research Institute of Fudan University in Ningbo, Zhejiang Province, China

ARTICLE INFO

Keywords:
Die attach
Sintered materials
Copper-matrix composite materials
Reliability
Power electronic packaging

ABSTRACT

While silver-based sintered materials are limited by cost and electromigration, and copper faces challenges with oxidation at high temperatures, Cu-based composite sintering materials offer promising alternative solutions. This review examines recent advances in Cu-based composite sintered materials for die-attach in power electronics packaging, focusing on their mechanical, thermal, electrical properties, and reliability. This review systematically categorizes such compounding strategies, including direct mixing, core-shell structures, and alloying, analyzing the impact on composite properties. Furthermore, the reliability of Cu-based composite sintered joints is evaluated, addressing high-temperature storage, thermal cycling, corrosion, and electrochemical migration. Challenges such as oxidation resistance, process optimization, and cost-effectiveness are discussed, together with future research directions. This work aims to support researchers in advancing Cu-based composite sintering materials research and development, broadening material options for high-temperature power electronics packaging applications.

1. Introduction

The rapid development of high-performance electronic devices, especially in electric vehicles, renewable energy, and aerospace, has led to an increase in power density and module miniaturization [1–3]. As a result, the demand for electronic packaging materials for efficient heat dissipation and mechanical integrity has grown dramatically [4]. The die-attach materials, bonding semiconductor chips to substrates, directly influence the device's thermal management, reliability, and longevity under extreme operating conditions [5].

Conventional solder materials have historically been the choices for die-attach applications due to their mature process and adequate bonding properties [6]. Lead solders, e.g., tin-lead (Sn–Pb) alloys, are facing environmental concerns such as the European Union's RoHS regulation [7,8], while lead-free solders, such as tin-silver-copper (SAC) alloys, suffer from limited performance for high-power and high-temperature applications [9,10]. Afterwards, silver (Ag)-based sintered materials have emerged as a promising alternative, offering superior thermal and electrical conductivity as well as excellent mechanical stability under high temperatures [11–15]. However, high costs and susceptibility to electromigration under high current densities continue to hinder their widespread adoption [16]. Nowadays, it begins to shift to copper (Cu) sintering, known for its cost-effectiveness and comparable thermal and electrical properties compared to silver sintering [15,17–19]. Nonetheless, copper's major drawback lies in its susceptibility to oxidation at elevated temperatures, leading to a loss in thermal conductivity and bond strength, thereby compromising its reliability in high-temperature environments [18,20].

To overcome these challenges, Cu-based composite sintered materials have garnered increasing attention for both research and industry [21–27]. These composites incorporate secondary elements such as silver, tin, or ceramics to enhance the oxidation resistance, thermal stability, and mechanical properties of copper, making it a viable candidate for high-performance die-attach applications [28].

As shown in Fig. 1, three primary strategies are commonly employed to optimize the performance of Cu-based composites:

* Corresponding author. College of Intelligent Robotics and Advanced Manufacturing, Fudan University, Shanghai, 200433, China.
E-mail address: panliu@fudan.edu.cn (P. Liu).

https://doi.org/10.1016/j.jsamd.2025.100963
Received 17 May 2025; Received in revised form 24 July 2025; Accepted 26 July 2025
Available online 5 August 2025

(1) ***Direct Mixing:*** This method blends copper with metallic or non-metallic fillers, such as silver or alumina, to enhance mechanical strength, improve thermal conductivity, and mitigate oxidation.
(2) ***Core-Shell Structures:*** Coating copper particles with a protective shell of oxidation-resistant material like nickel or silver provides a barrier that prevents surface degradation while maintaining high thermal and electrical conductivity.
(3) ***Alloying:*** The introduction of elements such as tin or bismuth into the copper matrix can improve its mechanical strength, sintering behavior, and thermal stability, making the material more suitable for high-temperature applications.

These strategies have proven effective in improving the properties of Cu-based sintered materials for the demanding requirements of power electronics. In addition to advances in processing techniques such as spark plasma sintering (SPS) and transient liquid-phase sintering (TLPS), simulation methods including finite element modeling (FEM) and molecular dynamics (MD) have been increasingly adopted to investigate thermal behavior, stress evolution, and microstructural development during sintering, thus bringing deeper understanding for sintering mechanism [29,30]. Simulation tools, combined with algorithms or artificial intelligence (AI) modelling, enable the optimization of material composition and processing parameters with limited experimental data, thereby accelerating the development of composites with enhanced thermal conductivity and mechanical integrity [31,32].

The adoption of Cu-based composite sintered materials in power electronics is promising for the future of high-performance packaging to withstand harsh conditions [33,34]. Cu-based composites not only address the shortcomings of traditional solder, pure copper, and silver-based sintering materials, but also provide a potential cost-effective and scalable solution for die-attach applications. While Cu-based composite pastes have attracted growing attention in emerging applications such as solar cell front electrodes and flexible printed electronics due to their excellent printability and conductivity, current reviews' efforts on power semiconductor packaging have rarely focused on the composite design and multifunctionality of Cu-based sintered materials [20].

Therefore, this review aims to provide a comprehensive overview of the advancements in Cu-based composite sintered materials for die-attach applications. Section 2 categorizes and evaluates the various strategies for material enhancement, focusing on the thermal, electrical, and mechanical properties of these composites. Section 3 delves into the research progress of the reliability evaluation of these materials under practical conditions, such as high-temperature storage, thermal cycling, corrosion, and electrochemical migration. Finally, Section 4 outlines the remaining challenges and proposes future directions for research, offering insights into how the development of Cu-based composites can revolutionize high-power electronic packaging.

2. Cu-matrix composite sintering materials

The development of copper-based sintered materials has undergone a continuous evolution driven by the growing performance requirements of high-power electronic devices, as shown in Fig. 2. Initially, pure copper sintering was explored as a cost-effective alternative to expensive silver-based pastes [35]. However, its high susceptibility to oxidation and poor long-term reliability limited its practical application.

To address these challenges, researchers have successively proposed several improvement strategies. Early efforts focused on direct physical blending with secondary metallic particles (e.g., Ag, Sn) or ceramic fillers to enhance thermal, electrical, and mechanical properties. This was followed by the introduction of oxide-assisted sintering, utilizing in-situ reduction of Cu_2O or CuO to improve interparticle bonding and densification. With advances in nanotechnology and interfacial engineering, core-shell structures such as Cu@Ag and Cu@Sn were developed to protect copper surfaces and enable low-temperature sintering while improving oxidation resistance. More recent approaches include polymer-assisted composites and nano-alloying designs enhance interfacial compatibility, processing flexibility, and environmental reliability. By 2023, research had shifted toward multi-component composite strategies, integrating various fillers and reaction control mechanisms (e.g., Cu/Ni-OPTG, Cu@Sn@Ag, Cu/Ag/Epoxy), to simultaneously optimize thermal, mechanical, and electrical performance. By 2025, the focus has expanded to include sintering mechanism modeling, interfacial reliability analysis, and multi-objective optimization tailored

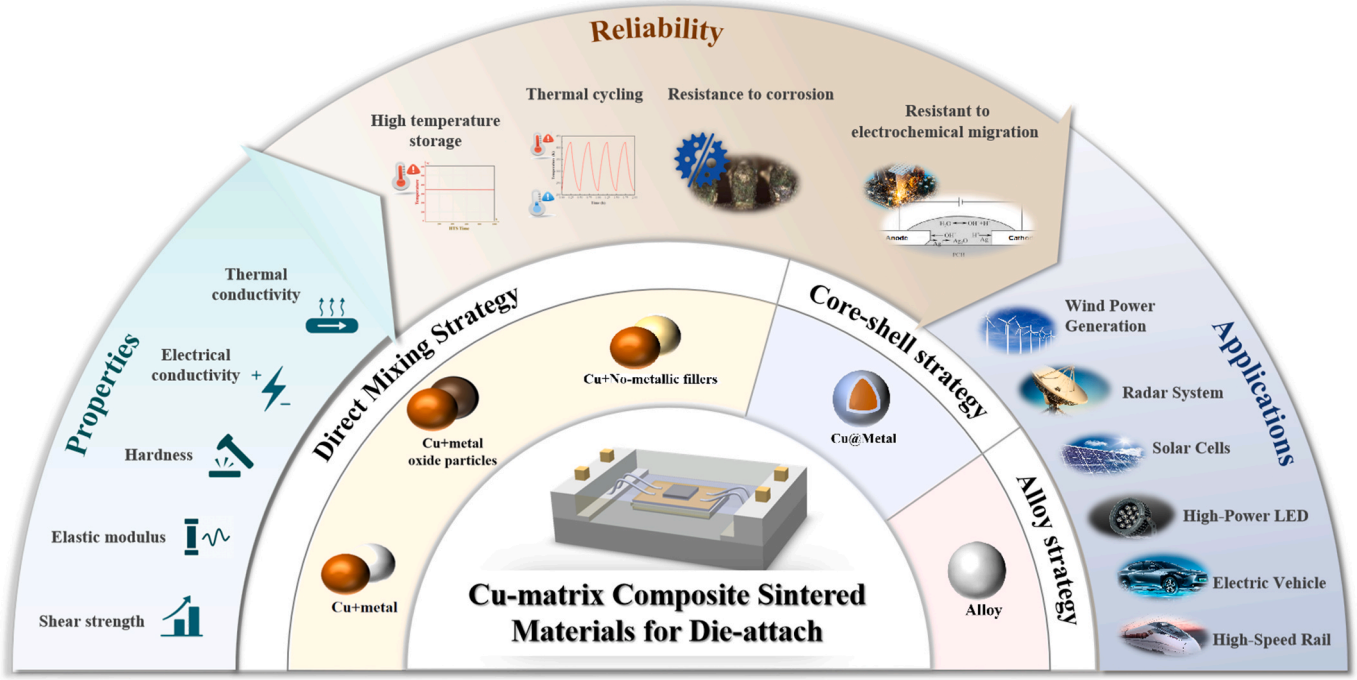

Fig. 1. Overview of challenges and strategies in the development of Cu-based composite sintered materials.

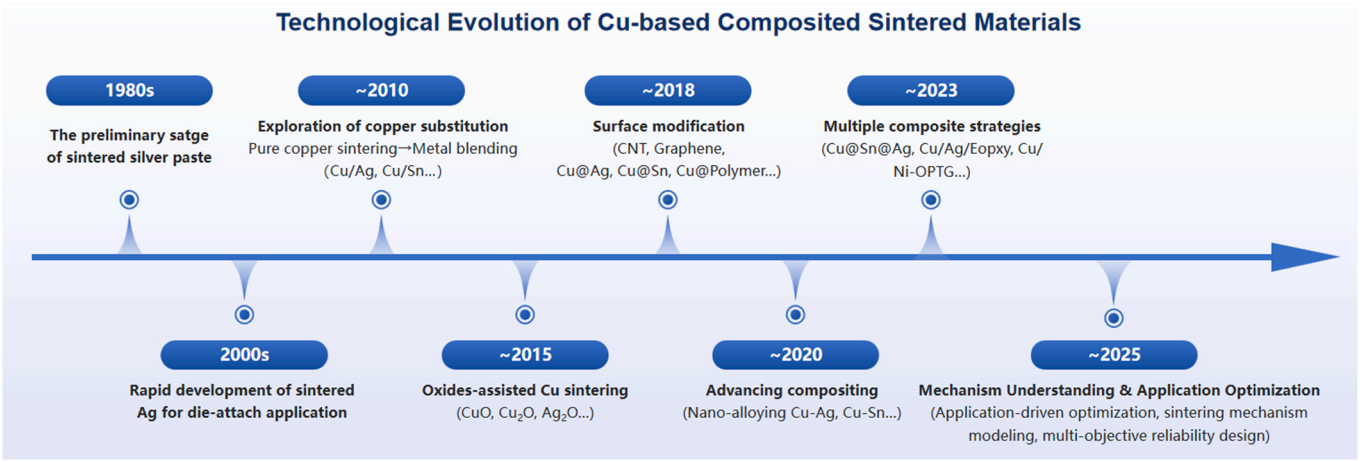

Fig. 2. Technological roadmap showing the key development stages of Cu-based sintered materials for electronic packaging applications.

to practical applications.

Against this background, the enhancement of Cu-based sintered materials has become a key research focus in electronic packaging, particularly as device integration density and thermal load continue to increase. Based on the evolution of material design strategies and composite methods, this section provides a systematic overview of Cu-based sintering paste development, which can be broadly categorized into three representative approaches: direct blending (Section 2.1), core-shell structuring (Section 2.2), and alloying (Section 2.3). Each method is analyzed in terms of processing techniques and performance characteristics.

2.1. *Cu-based blended composite materials*

The primary advantages of direct blending composite sintered copper materials lie in their simplicity and effectiveness in enhancing the performance of composite materials. This method involves the thorough mixing of different powders prior to the sintering process, ensuring even distribution of each component within the matrix. Through co-sintering, the resulting material exhibits improved mechanical properties, enhanced thermal and electrical conductivity, and increased resistance to environmental degradation. Moreover, direct co-sintering proves to be a cost-effective approach as it reduces the need for complex processing steps and utilizes readily available raw materials. The blended materials of Cu-based composite sintered materials can be categorized into three types: metallic materials (Section 2.1.1), metal oxide materials (Section 2.1.2), and non-metallic materials (Section 2.1.3). In the following sections, the performance and research advancements of Cu-based sintered joints following the combination of these three types of elements will be reviewed. Table 1 summarizes the preparation, properties, and high-temperature application potential of Cu-based blended composite sintered materials, focusing on the effects of copper-metal ratios, particle morphology, and sintering processes (including temperature, pressure, sintering time, sintering atmosphere, the metal particle size, etc.) on shear strength, porosity, hardness, modulus, and electrical and thermal conductivity. The entries in Table 1 are organized according to the type of secondary phase (metallic, metal oxide, and non-metallic materials) and further sorted chronologically by publication year within each category.

2.1.1. *Metallic particles*

Metallic particles serve as essential dopants in Cu-based composite sintered pastes, offering improvements in thermal conductivity, electrical properties, mechanical strength, and oxidation resistance. This section reviews key advancements and mechanisms associated with copper composites doped with silver (Cu + Ag), tin (Cu + Sn), and other metallic particles.

2.1.1.1. Cu + Ag. Copper-silver (Cu–Ag) mixed sintering materials have attracted considerable interest due to their excellent stability and outstanding performance in electronic packaging, especially for high-power device applications. As depicted in Fig. 3a, the Cu–Ag alloy phase diagram reveals a high level of stability between the two metals at temperatures below 300 °C, which inhibits the formation of intermetallic compounds (IMCs) under standard conditions. Since Kim et al. [36] introduced Cu–Ag nanopastes in 2014, researchers have been optimizing the Cu:Ag ratio, particle morphology, solvent systems, and sintering parameters. The related research progress is summarized in rows 1 to 9 of Table 1. From these studies, it can be observed that the primary research efforts have centered on tuning compositional ratios, tailoring particle structures, and incorporating functional solvents to improve densification and mechanical performance. Notable progress has been made in enabling low-temperature bonding, enhancing interfacial strength, and improving thermal and electrical conductivity through dual-scale filler design and epoxy-assisted sintering strategies. However, there is still a lack of in-depth understanding of the fundamental sintering mechanisms, including the dynamic interaction between Cu and Ag phases, interfacial bonding evolution, and porosity formation. These aspects remain underexplored and represent important directions for future investigation, particularly for applications requiring model-driven performance optimization and long-term reliability prediction.

The copper-silver ratio profoundly impacts the microstructure, electrical conductivity, and mechanical properties of Cu–Ag sintered materials. Cheng et al. [38] analyzed the sintering behavior of Cu–Ag composite particles and evaluated optimal Cu–Ag paste compositions using percolation theory, as shown in Fig. 3b. Their study revealed that a silver volume fraction of 75 % yielded optimal shear strength and resistivity under hot pressing, while a 35 % ratio sufficed for furnace sintering. Increasing silver content also reduces porosity and resistivity, as demonstrated by Lv et al. [40].

Particle morphology is another crucial factor that governs the properties of Cu–Ag sintered joints. Li et al. [22] introduced a multi-shape design for Ag–Cu bimetallic pastes, tailored for power electronic packaging applications. By leveraging the "rolling effect" of Cu spherical particles, silver flakes achieved a denser packing configuration, enhancing plastic deformation during sintering, as illustrated in Fig. 3c. This innovative design led to a notable improvement in the shear strength of sintered joints, showcasing the potential of morphology engineering in achieving superior material performance.

The choice of solvent significantly influences the dispersion of particles, sintering behavior, and overall performance of Cu–Ag composites.

Table 1
Summary of preparation methods and properties of Cu-matrix composite sintered materials.

Authors	Year	Materials	Processing	Porosity	Properties of the sintered joints					Ref.
					Shear Strength	Elastic Modulus	Hardness	Thermal Conductivity	Electrical Conductivity	
Kim et al.	2014	**Cu** (50 nm) + **Ag** (40 nm), Cu content: 20, 40, 50, 60, and 80 wt%	380 °C, 30 min, air, 1 cm × 1 cm	40.02 %–42.62 % (Cu content: 20–80 wt %)	/	/	/	/	0.81–2.27 × 10^5 $(\Omega\ cm)^{-1}$ (Cu content: 80~20 wt%)	[36]
Li et al.	2017	**Cu** (61.02 nm) + **Ag** (69.25 nm), 2:1 M ratio of Cu:Ag	250 °C, 1.12 MPa, 60 min, Ar–H_2 gas, 3 mm × 3 mm	/	25.41 MPa	/	/	/	1.99 × 10^{-7} Ω m	[46]
Guo et al.	2017	10/20 mol% **Cu** NP + **Ag NW** + **Ag NP** (Cu NP 100 nm, Ag NP 50–100 nm, Ag NW length 8–20 um/diameter 80 nm)	250 °C, 2–5 MPa, 10 min, air, diameter 6 mm	/	12~17 MPa	/	/	/	5.0 × 10^{-4} Ω m (20 mol% Cu NPs)	[47]
Liu et al.	2019	**Copper foam** + **Ag** (50 nm)	250 °C, 5 MPa, 5/10/15/20 min, 2 mm × 2 mm	/	25.51–41.77 MPa (5–20 min)	/	1.41–1.63 GPa (5–20 min)	/	/	[48]
Li et al.	2022	**S Cu** (1–3 μm) + **F Ag** (1–3 μm), content: Cu:Ag = 1:1	250 °C, 20 MPa, 300 s, N_2, 2 mm × 2 mm	/	47.42 MPa	/	/	/	/	[22]
Chen et al.	2023	**F Cu** (11.9 μm) + **Ag** amino complex; **S Cu** (10 μm) + **Ag** amino complex	180/250/300 °C, 30 min, air, 2 MPa, 3 mm × 3 mm/30 mm × 30 mm	/	16.9–56.7 MPa (180–300 °C, 3 × 3 mm); 31.9 MPa (300 °C, 90min, 5 MPa 30 × 30 mm)	/	/	138.3–243.7 W/m.K	/	[23]
Lv et al.	2023	**Cu** (9 nm) + **Ag**, with Cu and Ag atomic ratios of 3:1, 2:1, 1:1, 1:2, and 1:3	250 °C, Ar–H2 (5 % H_2) mixed atmosphere, 2 MPa, 3 mm × 3 mm	7.37 %–1.92 % (Cu3Ag ~ CuAg3)	22.8–32.6 MPa (Cu3Ag ~ CuAg3)	/	/	/	26.33–8.74 μΩ cm (Cu3Ag ~ CuAg3)	[40]
Cheng et al.	2023	**Cu** (1–10 μm) + **Ag** (0.1 μm), 25 %–85 % vol.Cu	250 °C, 30 min, air, 5 MPa, 5 mm × 5 mm	6.82 %–31.34 % (25 %–65 % vol.Cu)	1.36–8.88 MPa (65 %–25 % vol.Cu)	/	/	10.59–156.98 W/m.K (25 %–65 % vol.Cu)	7.80–18.60 μΩ cm (25 %–65 % vol.Cu)	[38]
Wang et al.	2024	**F Cu** (1–3 μm) + **F Ag** (1–3 μm), content: Cu:Ag = 1:1	250 °C, 20 MPa, 10 min, N_2, 2 mm × 2 mm	2.86 %	51.70 MPa	48.98 GPa	1.04 GPa	/	2.03 × 10^5 S cm^{-1}	[39]
Lang et al.	2013	**Cu** + **Sn**,<15 μm, content: Cu:Sn = 6:4	260 °C, 20 min, 0.3 MPa, N_2, 6.35 mm × 6.35 mm	/	~40 MPa	/	/	/	/	[41]
Greve et al.	2017	**S Cu** (37–88 μm) + **S Sn** (20–38 μm), content: Cu:Sn = 66 wt%:17 wt%	300 °C, 30 min, 0.3 MPa, 6.35 mm × 6.35 mm	<5 %	/	/	/	~140.2 W/m.K	/	[21]
Kato et al.	2017	**Cu** + **Sn-8 wt.% Cu** (<13 μm), content: Cu:Sn = 7:3	280 °C, 20 min, 0.1 MPa, N_2, 3 mm × 3 mm	~5 %	~42 MPa	/	/	0.13 W/K (Rth)	/	[49]
Said et al.	2020	**F Cu** + **Sn-0.7 Cu** (45 μm) content: Cu = 10 wt%	250 °C, 30 s	/	20.19 MPa	/	/	/	/	[50]
Yang et al.	2022	**S Cu** (0.9 μm) + **S Sn** (250 nm), content: Sn = 9/25/50 wt%	260 °C, 30 min, 5 MPa, 5 % H_2+95 % Ar, 3 mm × 3 mm	/	45/70/34 MPa (Sn = 9/25/50 wt%)	/	/	/	/	[42]
Shao et al.	2018	**Cu** (2 μm/20 μm)+ 20 μm-**thick pure Sn foil**	250/300 °C, 1–90 min, 0.3 MPa, diameter 6 mm	/	32.9 MPa (300 °C/45 min)	/	/	/	/	[31]
Min et al.	2021	**Cu** (4 μm) + **Sn–58Bi** (35 μm), Cu-50/70/90 Sn–58Bi	220 °C, 2 h, air, 3 mm × 3 mm	/	10.36/22.06/45.31 MPa (Cu-50/70/90 Sn–58Bi)	/	/	/	/	[44]
Siah et al.	2019	**Cu** + **Al** + **resin** (60–80 nm, content	380 °C, 30 min, 1 cm × 1 cm	/	/	/	/	/	21 μΩ cm	[43]

(*continued on next page*)

Table 1 (*continued*)

Authors	Year	Materials	Processing	Porosity	Properties of the sintered joints					Ref.
					Shear Strength	Elastic Modulus	Hardness	Thermal Conductivity	Electrical Conductivity	
		of Cu:Al = 8:2, 0.25 g resin)								
Greve et al.	2014	**Cu** + **Ni** + **Sn**	300 °C, 30 min, <0.5 MPa, 6.35 mm × 6.35 mm	/	Softening Behavior (shear strength<10 MPa) occurred >416 °C	/	/	/	/	[45]
Liu et al.	2016	flake-shape Cu particles with **Cu_2O** oxide layer, Formic acid as reducing solvent	0.08 MPa at 300 °C for 40 min	/	30.9 MPa	/	/	/	/	[51]
Yamagiwa et al.	2021	0.53 μm Submicron Cu particles, then with **Cu_2O** oxide layer	heated to 200–350 °C and held for 0.5–5 h under N_2-3 % H_2/N_2	12~14 %	N_2–3 %H_2:>20 MPa@ 300 °C, 350 °C; N_2: ≤6 MPa	/	/	/	/	[52]
Gao et al.	2020	**Cu** particles, **Cu oxide** fragments, **Cu** oxide nanoparticles; Formic acid as reducing solvent	~0.07 MPa at 300 °C for 10/20/30/40 min;	/	7~27 MPa	/	/	/	/	[53]
Gao et al.	2019	flake-shaped Cu microparticles (6.9 μm) with **Cu_2O** nanoparticles (after ORB)	under formic acid atmosphere at 300 °C with Cu/Ag/Au substrates	/	Cu: 14.89–17 MPa; Ag:17.34–30.28 MPa; Au:23.57–35.10 MPa	/	/	/	/	[25]
Ogura et al.	2013	**Ag_2O: CuO** mixed at a weight ratio of 9:1; PEG 400 as reducing solvent	5 MPa from 300 °C to 400 °C for 300 s	/	31–50 MPa from 300 °C to 400 °C	/	/	/	/	[54]
Han et al.	2023	**Cu: Ag_2O** mixed at a weight ratio of 4:6/3:7; glycerol, EW-10 as reducing solvent	5 MPa at 300 °C for 300 s	3:7–4.52-0.09 % for 300s	10.6–38 MPa (4:6) 27.8–45.5 MPa (3:7)	/	/	/	/	[55]
Yao et al.	2018	**CuO** particles (1 μm); PEG1000 as reducing solvent	5/10/15 MPa at 300/350/400/450/500 °C for 15 min;	/	5.7–24 MPa	/	/	/	/	[56]
Hou et al.	2021	gas atomized copper powders (5–70 μm) with **Cu_2O** nanoparticles (after ORB)	5/7.5/10/12.5/15 MPa at 300 °C in a formic acid atmosphere for 40 min	/	20.7–32.9 MPa	87~93 GPa	1.86–2.15 GPa	/	/	[57]
Park et al.	2014	**Cu/CuO/Cu_2O** equiaxed flakes; DN/EG/DEG/TEG/PEG as reducing solvent	0.4 MPa at 300 °C for 60 min; 4 mm × 4 mm	/	9.6, 13.2, 9.8, 16.4 MPa	/	/	/	/	[58]
Matsuda et al.	2023	**Cu_2O** nanoparticles; PEG 400 as reducing solvent	5 MPa, 260–300 °C held for 30 min	/	<15 MPa at 260 °C, >30 MPa at 280, 300 °C	/	/	/	/	[59]
Zuo et al.	2020	0.1 μm **CuO** particles; ascorbic acid and ethylene glycol, glycerol, PEG as reducing agent I, II, III	3 MPa at 220 °C for 10/15/20/40/80/240 min;	/	reach a peak of 22 MPa at 15 min	/	/	/	/	[60]
Gao et al.	2018	As-synthesized **Cu** particles (**Cu@Cu oxide**); 0/5/10/15 wt% AA dissolved in EG as solvent	0.4 MPa from 200 °C to 350 °C for 30 min; N_2	/	14.4 MPa with 0 wt % AA at 350 °C; 24.8 MPa with 10 wt% AA at 300 °C	/	/	/	/	[61]
Siah et al.	2019	**Cu** + **Al** + **resin** (60–80 nm, content of Cu:Al = 8:2, 0.25 g resin)	380 °C, 30 min, 1 cm × 1 cm	/	/	/	/	/	21 μΩ cm	[43]
Wang et al.	2024	**F Cu** (1–3 μm) + **F Ag** (1–3 μm) + **epoxy resin** (5–10	250 °C, 20 MPa, 10 min, N_2, 2 mm × 2 mm	1.93 % (5 wt% epoxy)	48.54 MPa (5 wt% epoxy)	27.37 GPa (5	0.69 GPa (5 wt% epoxy)	/	1.336×10^5 S cm^{-1} (5 wt% epoxy)	[39]

(*continued on next page*)

Table 1 (*continued*)

Authors	Year	Materials	Processing	Porosity	Properties of the sintered joints					Ref.
					Shear Strength	Elastic Modulus	Hardness	Thermal Conductivity	Electrical Conductivity	
		wt%), content: Cu: Ag = 1:1				wt% epoxy)				
Wang et al.	2023	**F Cu** (1–3 μm) + **epoxy resin** (5 wt %)	250 °C, 20 MPa, 15 min, N_2, 2 mm × 2 mm	/	36.25 MPa	/	/	/	/	[34]
Hwang et al.	2021	**S Cu** (4 μm) + **F Cu** (20 μm) + **resin** (5, 10, 15 wt%), content: S Cu:F Cu = 1:1	250 °C, 30 min, N_2, 3 mm × 3 mm	/	2.81, 12.1, 16.23 MPa	/	/	/	1.74, 1.88, 3.03 Ω (5, 10, 15 wt% resin)	[24]
R.Vignesh et al.	2019	**Cu** + **CNTs** (diameter 10–60 nm, length 10 μm, content: 0.25~1 wt %)	600 °C, 60 min, N_2	/	/	/	69~81.2 VHN (CNT 0.25 wt%)	314~328 W/mK (CNT 0.25 wt%)	42.5–44.4 MS/m (CNT 0.25 wt%)	[62]
Wu et al.	2022	**Cu** (spherical particles 20–60 nm, 0.2–0.6 μm and 1–2 μm) + **MWCNTs** (content: 0~1.2 wt %)	300 °C, 5 MPa, 30 min, Ar–H_2, 10 mm × 10 mm	/	26.64 MPa (0.6 wt % MWCNT, 85 % H_2+15 % Ar)	/	/	/	3.571 μΩ cm	[63]
Gutierrez et al.	2017	**Cu** (10 μm + 15 nm) + **SiC@Ag** (0.5–4 wt%)	500 °C, 6.5 MPa, 30 min, N_2, 2 mm × 2 mm	/	/	/	/	52.2 W/mK	/	[64]
Yang et al.	2025	**Cu** (300 nm) + **Ni-OPTG** (0.1 wt%)	255 °C, 5 MPa, 30 min, Ar–H_2, 3 mm × 3 mm	/	56.26 MPa	/	/	216.2 W/mK	/	[65]

Wang et al. [39] demonstrated that modifying solvents by incorporating epoxy resin greatly improved the shear strength of sintered joints, as presented in Fig. 3d. This effect was particularly evident after high-temperature storage and thermal cycling, highlighting the role of solvent chemistry in enhancing material reliability under extreme conditions.

The parameters of the sintering process include temperature, pressure and time, which play decisive roles in determining the final properties of the copper-silver mixed sintered material. Chen et al. [23] achieved shear strength up to 56.7 MPa and thermal conductivity of 243.7 W/m·K at 300 °C and 2 MPa, rivaling Ag-based pastes, as shown in Fig. 3e. These findings highlight Cu–Ag systems' potential for cost-effective, high-performance packaging.

2.1.1.2. Cu + Sn. Tin (Sn) particles, alongside silver, are commonly used fillers in Cu-based sintered composites, primarily to enhance wettability and filling properties. Due to its low melting point, Sn acts similarly to solder in the composite, facilitating sintering at relatively low temperatures. Early research of Lang et al. [41] in 2013 demonstrated that a mixed sintered material consisting of 60 % Cu and 40 % Sn exhibited a shear strength of approximately 40 MPa under low-pressure-assisted sintering conditions, making it an ideal candidate for power electronics packaging. However, in the Cu–Sn phase diagram (Fig. 4a), Cu and Sn can form various intermetallic compounds (IMCs), which have a pronounced impact on the final properties of the materials during the sintering process. Major Cu–Sn IMCs include Cu_6Sn_5 (η phase) and Cu_3Sn (ε phase), with melting points of 415 °C and 676 °C, respectively. During sintering, Sn melts first due to its low melting point (232 °C), and subsequently reacts with Cu particles to form Cu–Sn IMCs, resulting in potential phases such as unreacted Cu, Cu_6Sn_5, Cu_3Sn, and possibly Cu–Sn solid solutions.

Rows 10 to 15 of Table 1 summarizes the current research progress on Cu–Sn mixed sintering. Comparative analyses reveal that particle size, morphology, mixing ratio, and sintering conditions play decisive roles in determining the density, microstructure, and mechanical properties of the sintered joints. These studies highlight progress in tailoring filler characteristics and sintering parameters to achieve improved joint performance, particularly through the use of hierarchical particle sizes and transient liquid phase sintering (TLPS) techniques. However, research on the dynamic formation and evolution of Cu–Sn IMCs during sintering, especially under rapid or pressureless conditions, remains limited. In-depth studies are still needed to fully understand interfacial reaction kinetics and IMC layer morphology.

Particle size and morphology critically influence sintering density and microstructural evolution. Larger Cu particles create effective flow channels for molten Sn, which enhances densification and mechanical properties. Shao et al. [31] demonstrated that porous Cu layers combined with Sn foils achieved enhanced densification through capillary action, resulting in robust Cu–Sn joints, as exhibited in Fig. 4b. Additionally, the use of nano-sized Sn particles in TLPS pastes improved in sintering efficiency and joint reliability [42].

The ratio of Cu to Sn particles determines the phase composition and mechanical properties of the sintered product. Optimal Sn content (~25 wt%) promotes Cu_3Sn formation and enhances strength, as shown by Yang et al. [42] (Fig. 4c). The results indicated that adequate Sn content promoting the formation of Cu_3Sn IMC are improving joint strength, while excessive Sn content may lead to the formation of Cu_6Sn_5 IMC which could weaken the joint.

The sintering temperature and time influence the formation of IMCs and joint strength in Cu–Sn systems. Moderate heating (e.g. 260 °C) ensures thermal stability [41]. Prolonged sintering enhances IMC uniformity and shear strength, though excessive duration offers limited benefits. Shao et al. [31] found that increasing the sintering duration from 5 to 15 min resulted in a 25 % increase in shear strength, attributed to the enhanced uniformity of the Cu_6Sn_5 phase. However, excessive time yielded diminishing returns, as presented in Fig. 4d. Additionally, while appropriate pressure enhances densification, excessive force may cause structural damage. Therefore, careful optimization is crucial for achieving reliable and cost-effective manufacturing.

2.1.1.3. Cu + Others. Researchers explored the combination of other materials or multi-component mixtures to develop novel bonding

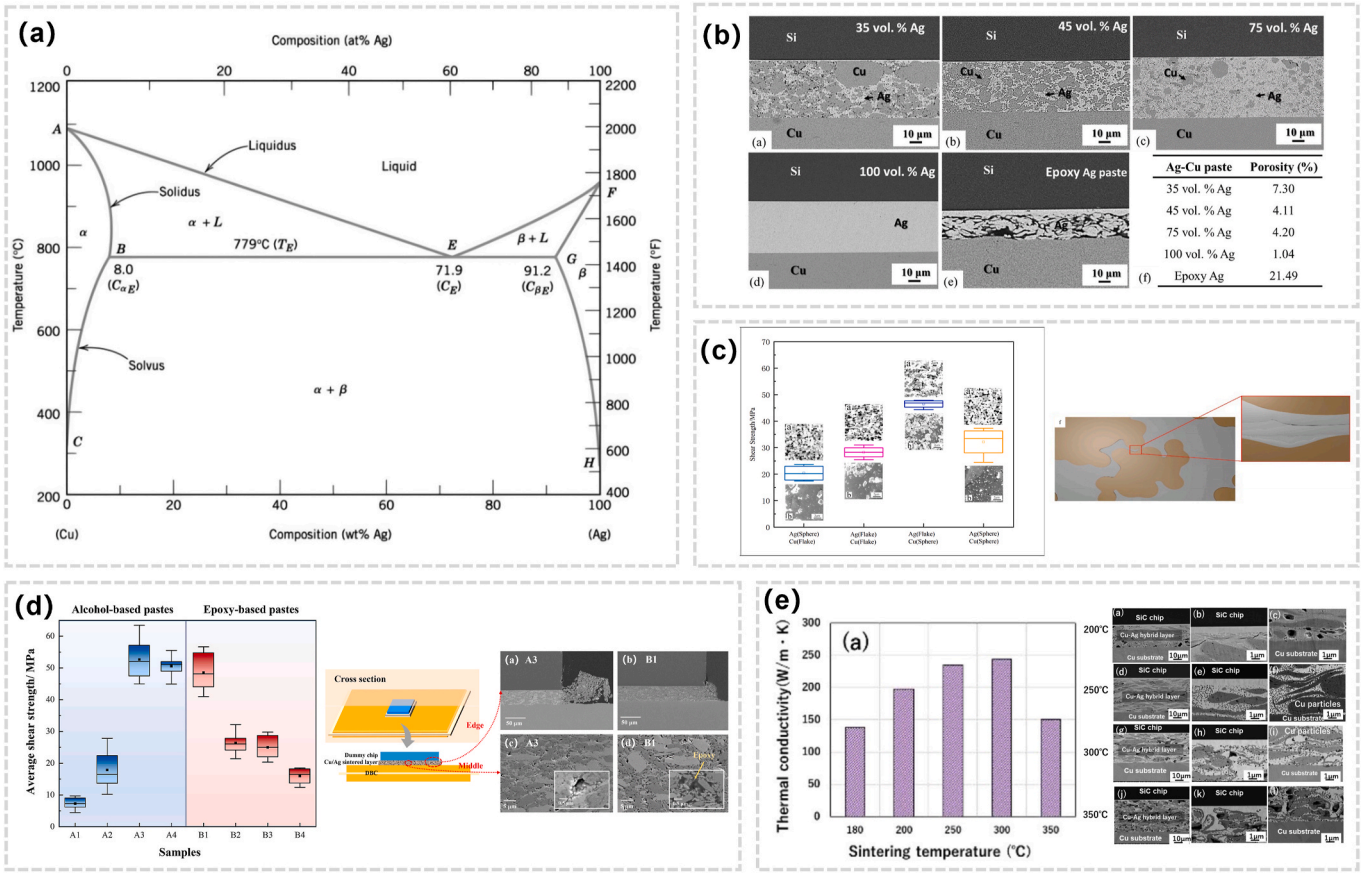

Fig. 3. Research progress of Cu–Ag sintering pastes. (a) Copper-Silver Phase Diagram [37]; (b) Cross-sectional SEM–BSE images and depicted porosity values of 35~100 vol% Ag–Cu pastes bonded with a Si chip and Cu substrate after tube furnace bonding at 250 °C for 30 min in an Ar atmosphere [38]; (c) Die shear strength of four types of sintering pastes and sintering mechanism illustration of Ag flake - Cu sphere paste. (d) Average shear strength of sintered samples and SEM morphology photos of the edge and middle of the A3 and B1 sample [39]. (e) Results of the room-temperature thermal conductivity of the sintered Cu–Ag paste at the different sintering temperatures and BSE image of the cross-section of the SiC–Cu joint structure using Cu–Ag paste at 200 °C, 250 °C, 300 °C, and 350 °C, respectively [23].

materials capable of stable operation at higher temperatures, listed in rows 16 to 18 in Table 1. For instance, Siah et al. [43] showed that Cu–Al systems formed $CuAl_2$ with low resistivity at 380 °C. From these studies, it is evident that the introduction of alternative metals, such as Al, Bi, or Ni, has expanded the range of achievable properties in Cu-based systems. These efforts have led to notable progress in lowering sintering temperatures, improving joint stability, and enhancing performance under thermal stress. However, current research remains limited in terms of in-depth mechanistic understanding of multi-element alloying effects, particularly concerning IMC evolution, thermal fatigue behavior, and long-term oxidation resistance in real application scenarios.

Furthermore, the incorporation of another metal element into the Cu–Sn system represents a promising strategy for enhancing the properties of the material. In the Cu–Sn–Bi system, researchers have attempted to reduce the sintering temperature by adding Bi. For instance, Min et al. [44] found that the addition of Bi reduced sintering temperature and stabilizes joints via Cu_3Sn formation. In a separate investigation, they explored the use of TLPS technology with Cu and Sn–58Bi alloys, successfully achieving Cu–Cu bonding at 220–270 °C with improved corrosion and thermal resistance. Additionally, Greve et al. [45] developed a TLPS paste composed of Ni, Cu, and Sn, which demonstrated a higher melting point following low-temperature processing and exhibited exceptional mechanical properties and fatigue resistance in high-temperature environments.

In conclusion, different particle processing parameters, including particle size, morphology, mixing ratio, and sintering process, all evidently influence the sintering behavior of these Cu-metal particle mixed systems. With the development of copper composites doped with silver (Cu + Ag), tin (Cu + Sn), and other metallic particles, it demonstrated that the co-sintering technology of copper with other metals not only enhanced the performance of electronic packaging materials under high-temperature working conditions but also provided new possibilities for the development of future high-temperature electronic devices. These findings provide valuable data and theoretical support for the research of electronic packaging materials, laying a foundation for further material optimization and process improvement.

2.1.2. *Metal oxide particles*

Copper nanoparticles are anticipated to serve as a cost-effective alternative to high-lead solder. However, during synthesis and storage, copper particles tend to agglomerate and oxidize, which degrades the performance of joints formed by conventional sintering. To overcome these limitations, researchers have developed an “in-situ reduction sintering” approach: copper oxide is first dispersed in the paste, then converted to elemental copper via a reduction reaction during sintering. This technique not only neutralizes the detrimental effects of surface oxides but also enhances interparticle bonding strength and overall joint density. For instance, Liu et al. [51] first generated Cu_2O by oxidizing copper in air at 300 °C, then introduced formic acid vapor into the sintering furnace to reduce the oxide in-situ according to the reaction:

$$Cu_2O + HCOOH(g) \rightarrow 2Cu + H_2O(g) + CO_2(g) \quad (1)$$

As shown in Fig. 5a and b, joints produced by such in-situ reduction

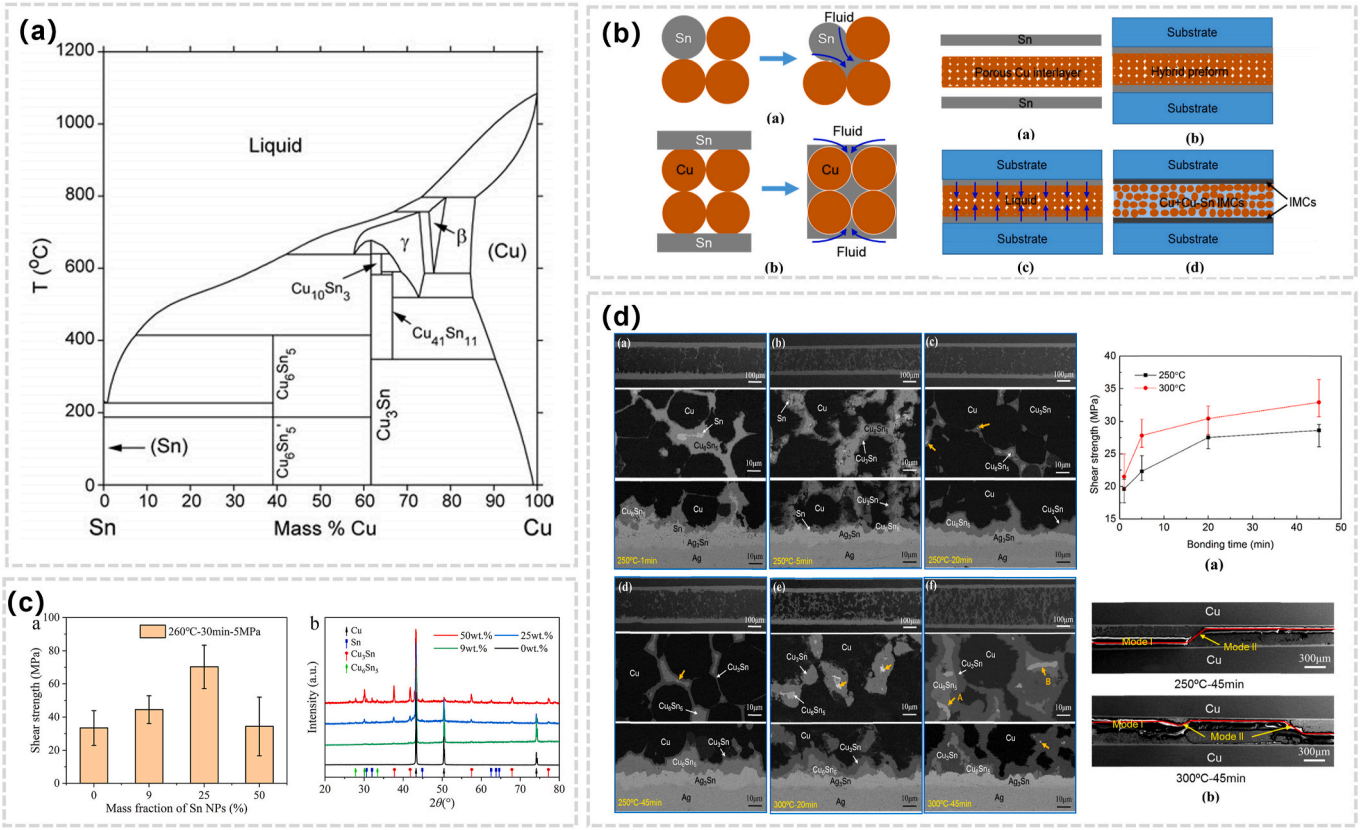

Fig. 4. Research progress of Cu–Sn sintering pastes. (a) Copper-Tin Phase Diagram [41]; (b) Schematic diagram of the microstructure densification in TLP sintering and this method. And schematic diagram of the novel TLP bonding totally through capillary action [31]; (c) Shear strength and XRD patterns of the sintered joints of Cu–Sn paste with different mass fractions of Sn [42]; (d)Micrographs (backscattered-electron (BSE) images)and shear strength of the joints bonded at different temperatures and time [31].

process reached shear strengths up to 30.9 MPa, substantially higher than those of conventional high-lead solders, mainly due to the nano-textured surfaces of the copper particles. In a similar approach, Yamagiwa et al. [52] used hydrogen as the reducing agent to pressurelessly sinter a Cu_2O + Cu mixed paste, generating copper nanoparticles directly within the joint. The high specific surface energy of these newly formed nanoparticles drives them to "bridge" interparticle voids, thereby enhancing particle aggregation and sintering and yielding shear strengths above 18 MPa. Gao et al. [25] took this concept further by ball-milling a composite paste of Cu_2O nanoparticles and Cu microparticles (Fig. 4c) and then pressurelessly sintering it. Their study demonstrated that the Cu_2O nanoparticles filled the gaps between microparticles and reduced in-situ to copper, which densifies the bonding layer and achieves an average shear strength of 23 MPa [53].

In addition to CuO/Cu_2O–Cu composite paste, Ag_2O–Cu composite pastes have also proven highly effective. Han et al. [55] prepared a paste with a Cu:Ag_2O mass ratio of 3:7 and performed in-situ reduction sintering under 5 MPa for 30 s and 90 s, achieving shear strengths of 27.8 MPa and 41.9 MPa, respectively. Microscopic analysis showed that gaseous by-products released during Ag_2O reduction promote uniform densification of the sintered layer, further boosting bond integrity. The in-situ reduction of Ag_2O follows the reaction:

$$5Ag_2O + C_2H_4(OH)_2 \rightarrow 10Ag + 2CO_2 + 3H_2O \quad (2)$$

Yao et al. [56] highlighted that the reduction temperature, as well as the choice of the reducing agent, directly influenced the shear strength of the Cu–Cu bonds. Table 2 summarizes the key advantages and disadvantages of typical reducing agents for sintering Cu-based oxides, including hydrogen, formic acid, polyethylene glycol (PEG), glycerol, and ascorbic acid (AA), for sintering Cu-based oxides. Although a hydrogen atmosphere features a lower activation energy for CuO reduction (≈60.7 kJ/mol) [66] than formic acid (≈97.4 kJ/mol) [67], with faster kinetics and more complete oxide removal, the extreme flammability, explosion risk, and high cost have limited its industrial adoption. As a result, formic acid remains the prevailing gas-phase reducer despite its higher energy barrier. To mitigate these safety and cost concerns, researchers have turned to in-situ liquid-phase reducing agents. For example, adding PEG to a Cu/CuO paste enables in-situ reduction of CuO to Cu during sintering, yielding joints with excellent mechanical integrity [56,58,59]. Zuo et al. [60] further demonstrated that glycerol outperforms PEG in reduction efficiency and leaves no residual organics, thereby promoting better particle densification. Ascorbic acid (AA) offers both self-reducing and self-protecting capabilities. Its decomposition products (CO, CH_4, and HCOOH) continue to reduce metal oxides throughout the sintering process [61].

In summary, in-situ reduction sintering has emerged as a breakthrough technique for overcoming the oxidation and agglomeration challenges of copper nanoparticles, with relevant studies summarized in rows 19–30 of Table 1. By combining formic acid or hydrogen reduction, mechanical grinding to enhance interparticle bonding, and copper-oxide/composite paste strategies, researchers have achieved improvements in joint performance, such as shear strength over 45 MPa. However, despite the promising results, current studies remain limited in several key aspects, which are critical for further advancing this technique. These include the lack of systematic investigation into reduction kinetics, limited understanding of byproduct effects (e.g., gas release and porosity formation), and insufficient real-time monitoring of oxide-to-metal transformation during sintering. Moreover, most studies rely on empirical optimization, while predictive models for reduction efficiency and interfacial evolution are still lacking. These gaps highlight the need

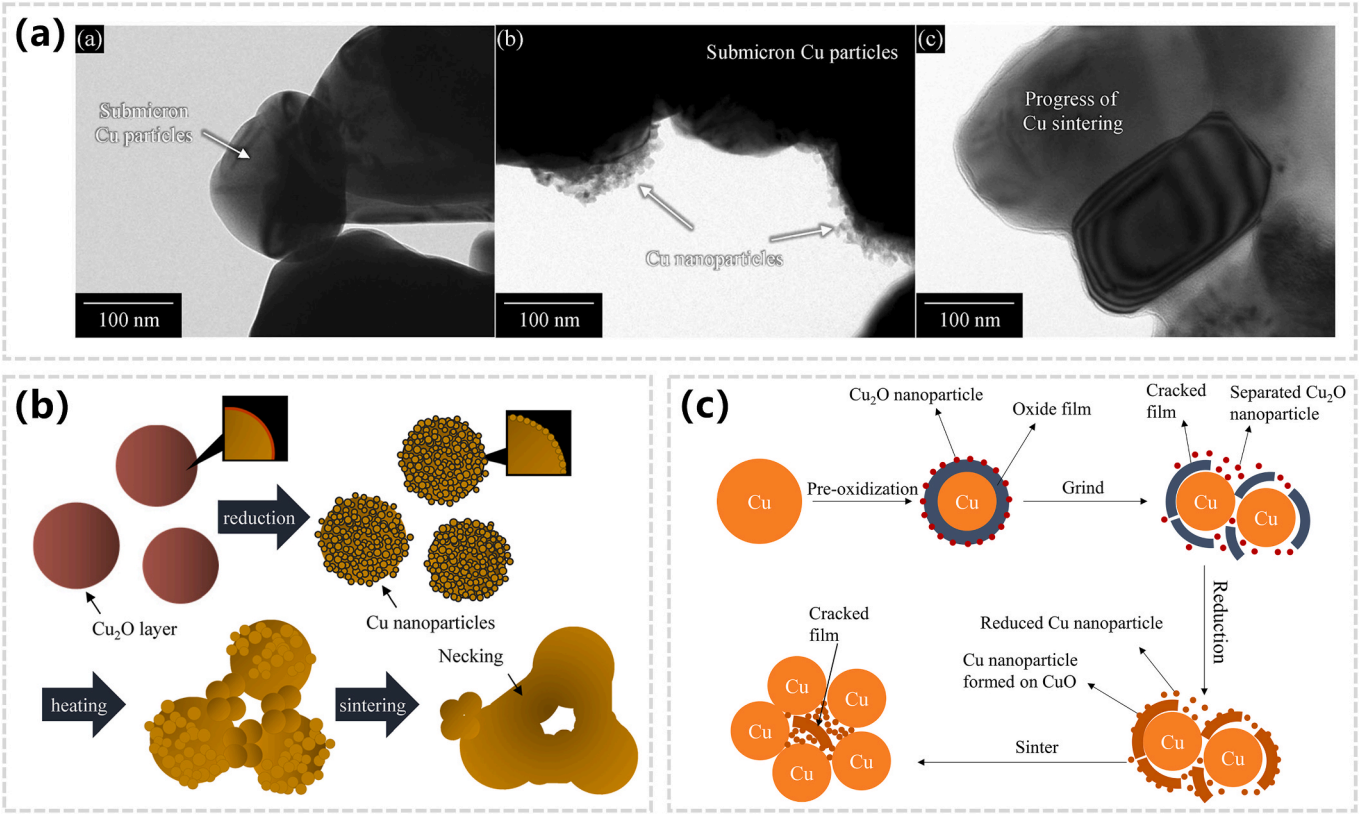

Fig. 5. Morphological changes and mechanisms of sintering behavior of oxidized copper particles: (a) TEM images of particles of submicron Cu paste heated up to 200 °C, 250 °C and 300 °C [52]. (b) Schematic diagram of the sintering process of submicron Cu paste [52]. (c) The schematic of the pre-oxidation ORB method (Oxidation-Reduction-Bonding method) with a grinding step [25].

Table 2
Comparisons of various reducing agents in Cu-based $CuO/Cu_2O/Ag_2O$ sintering.

Reducing agent	Advantages	Disadvantages	Ref.
Formic acid (g)	Controllable, eco-friendly (products: CO_2, H_2O)	Toxicity, corrosive to devices	[25, 51,53, 57]
H_2 (g)	Impurities-free (products: H_2O)	Potential explosions, high cost	[52]
Polyethylene glycol (l)	Low cost, easy to prepare	Incomplete evaporation, with organic residues hindering sintering.	[54, 56,58, 59]
Glycerol (l)	Low cost, low reduction temperature	Limited industrial application; longer reduction time	[55, 60]
Ascorbic acid (l)	Low cost, self-protection, without biohazards	Limited reductive capacity at high oxide concentrations	[61]

for deeper mechanistic insight, which is essential for the rational design and broader application of in-situ reduction strategies. Although this discussion has focused on the in-situ reduction of copper oxides, oxide-assisted sintering methods have become integral to hybrid copper-based material systems, enabling the fabrication of high-performance sintered composites through reinforced interparticle bonds.

2.1.3. *Non-metallic fillers*

Non-metallic fillers are becoming increasingly prevalent in Cu-based composites as a means of enhancing various material properties, such as thermal conductivity, mechanical strength, and thermal fatigue resistance. Particularly, resin filling, carbon nanotube (CNT) filling, as well as Cu-WC and Cu-graphite composites fabricated using the novel spark plasma sintering (SPS) process, have been explored as potential solutions.

Firstly, epoxy resin has been utilized in various applications, such as epoxy solders, underfill materials, and epoxy molding compounds, to augment mechanical adhesion and offer protection for filler substances in electronic packaging. When incorporated into Cu-based pastes for die-attach, epoxy serves as a flexible bridge between rigid particles, enhancing joint strength and mitigating crack formation. However, a major challenge lies in balancing mechanical reinforcement with thermal conductivity retention. For example, Siah et al. [43] demonstrated that resin additives not only improved the microstructure and bond strength of Cu–Al nanopastes under pressureless sintering at 380 °C, but also evidently reduced electrical resistivity. Inspired by such studies, Hwang et al. [24] formulated hybrid Cu pastes with varying epoxy contents (0–15 wt%) and conducted heat-curing treatments. As shown in Fig. 6a, adding 10 wt% epoxy improved shear strength to 12.1 MPa while maintaining acceptable resistivity, owing to gap-filling effects and strengthened filler bonding at lower temperatures and pressures. Similarly, Wang et al. [34,39] introduced epoxy into Cu and Cu–Ag sintering pastes and evaluated the microstructure and mechanical properties using SEM and nanoindentation. The epoxy-modified pastes exhibited enhanced gas barrier properties, reduced porosity, and improved microstructural homogeneity. In a complementary study, Wang et al. [69] employed finite element modeling to predict electrical, thermal, and thermomechanical behavior, supported by SEM/EDS image recognition, providing valuable insights for process optimization and paste formulation.

Secondly, carbon-based materials, including carbon nanotubes, graphene, and carbon fibers, are widely utilized in Cu-based composites due to their exceptional mechanical strength, electrical conductivity, and thermal conductivity. Carbon nanotubes (CNTs), being nanomaterials characterized by high strength and modulus, effectively enhance the mechanical properties of composite materials. Research

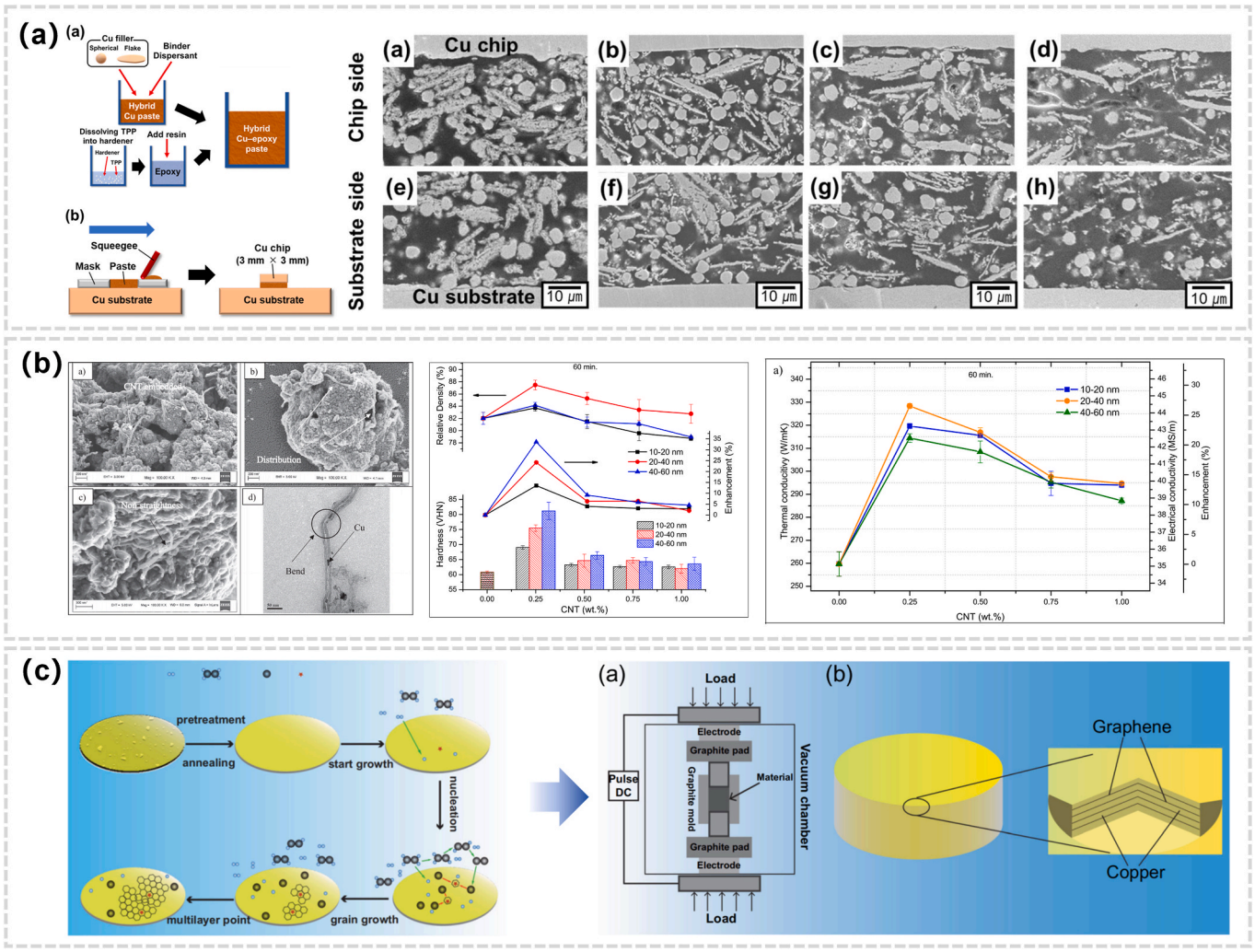

Fig. 6. Research progress of Cu-non-metallic sintering pastes.(a) Schematic diagrams of a hybrid Cu-epoxy paste fabrication process and cross-sectional microstructure of Cu–Cu joint with x wt% epoxy (x = 0, 5, 10, or 15) [24]; (b) Cu/CNT composite powder having 1 wt% of 40–60 nm CNT embedded in Cu, 20–40 nm CNT in Cu matrix, 10–20 nm CNT in Copper matrix, and 10–20 nm CNT with different types of defects obtained from TEM. And hardness and its enhancement, the relative density, electrical and thermal conductivity of sintered Cu/CNT composites [62]. (c)Schematics of the graphene formation during the CVD process with copper foil as a substrate, the SPS process and copper matrix-graphene layered composites [32,68].

conducted by R. Vignesh demonstrates that when used as fillers, CNTs can enhance the thermal conductivity and hardness of copper, particularly when the concentration is below 1 %, as shown in Fig. 6b [62]. These enhancements primarily rely on the diameter and distribution of the carbon nanotubes within the copper matrix. Regardless of their diameter, the greatest improvements in performance are achieved at a CNT concentration of 0.25 wt%, resulting in a thermal conductivity of 328 W/mK and a hardness of 81.2 ± 2.9 VHN for CNT composites with a diameter of 40~60 nm. Similar studies indicate that incorporating multi-walled carbon nanotubes (MWCNTs) into a copper matrix effectively enhances the tensile strength and stiffness of the material. Wu et al. [63] successfully improve the mechanical and electrical properties of Cu–Cu joints, particularly the bonding strength and resistivity, by introducing functionalized MWCNTs. Furthermore, functionalized MWCNTs have a positive impact on joint reliability, attributed to their ability to enhance the affinity between copper and carbon nanotubes, thereby increasing the bonding layer's density. Oxygen-containing functional groups, particularly carboxyl groups, have been found to enhance the interfacial bonding between Cu and CNTs, as reported by Park et al. [70]. Wu et al. [63] report an enhancement in shear strength from 23.4 MPa to 26.64 MPa through the incorporation of 0.6 wt% nitrogen-doped multi-walled carbon nanotubes (N-doped MWCNTs) into copper paste. The resistivities of the sintered Cu/N-doped MWCNTs layer and the Cu/carboxylated MWCNTs are measured at 2.252 μΩ cm and 2.551 μΩ cm, respectively. These values are substantially lower than the resistivity of the sintered pure copper layer, which is 3.473 μΩ cm, thus indicating superior electrical properties.

Moreover, graphene, a two-dimensional carbon material, has garnered considerable attention for its potential application in Cu-based composite materials. This interest stems from its high specific surface area and exceptional electrical and thermal conductivity. Research has indicated that the addition of graphene in small amounts to a copper matrix leads to notable improvements in the thermal conductivity and oxidation resistance of the composite materials. Additionally, the employment of SPS technology enables high-density sintering at lower temperatures and shorter durations, thus preserving the original characteristics of the filler material. As illustrated in Fig. 6c, optimized SPS parameters yielded composites with excellent mechanical strength and corrosion resistance, especially in high-temperature applications [32, 68]. Recently, further studies have extended the application scope of graphene-based fillers. Wei et al. [71] developed a silver/graphene oxide composite using a dual-dispersion medium method, which exhibited high thermal and electrical conductivity along with excellent mechanical performance. Subsequently, Yang et al. [65] extended it to

the preparation of nickel nanoparticle-decorated graphene/copper composites and reported enhanced interfacial bonding and heat dissipation properties, attributed to the synergistic effect of Ni and graphene layers. These results highlight the unique role of graphene in reducing porosity, promoting densification, and suppressing nanoparticle agglomeration during sintering. Such findings further support the potential of graphene as a material with a negative thermal expansion coefficient and its derivatives in advancing high-performance sintered composites.

In conclusion, non-metallic fillers serve as critical tuning components in Cu-based sintering systems. The detailed properties of sintered materials with different non-metallic fillers are shown in the last 10 rows of Table 1. As shown in the table, materials such as epoxy, CNTs, and graphene demonstrate excellent compatibility, wettability, and dispersion behavior, enhancing powder formability and sintered joint density. These advantages make non-metallic fillers particularly valuable for high-performance electronic packaging under harsh conditions (e.g., high temperature, humidity, and corrosive environments). However, the diverse effects of different fillers necessitate further optimization of filler content, morphology, and sintering parameters. Ongoing research continues to explore their full potential in advancing Cu-based composite sintering pastes for next-generation applications.

2.2. Cu@- core-shell particles based composite materials

Composite additives have shown great potential in enhancing the performance of Cu-based sintered materials, while challenges such as weak interfacial adhesion with materials like silicon carbide, high-temperature oxidation, and poor stability in humid or corrosive environments still persist [72]. Cu-based core-shell structures offer a promising solution by uniformly encapsulating copper particles with a shell material. Such a core-shell design improves microscale uniformity, enhances interfacial bonding, aligns thermal expansion coefficients with substrates, and prevents uneven powder distribution and local performance variability. The low-melting-point shell promotes the formation of a transient molten phase during sintering, enabling high-density, high-strength sintered bodies at lower temperatures [73], while corrosion-resistant shells like nickel or gold protect against oxidation and ensure long-term reliability under harsh conditions. By leveraging electrochemical principles, the core-shell structure effectively mitigates oxidation and chemical corrosion [74], making it well-suited for high-performance electronic packaging applications requiring precise control over material properties and sintering behaviors.

2.2.1. Synthesis methods of Cu-based core-shell structures

The synthesis of Cu-based core-shell structures is broadly categorized into metal coating and non-metal coating approaches. To achieve precise control over particle size, morphology, and shell thickness, researchers have developed and refined various synthesis techniques.

2.2.1.1. Metal coating. For metal-coated structures, the primary synthesis methods include liquid phase reduction and chemical plating:

- *Liquid Phase Reduction*: Copper core particles are suspended in a solution containing metal salts. Reducing agents, such as sodium borohydride or ascorbic acid, are employed to deposit a uniform metal shell onto the copper cores [75–77], as shown in Fig. 7a. This technique is simple, scalable for large-scale production. It also allows precise control over shell properties by adjusting parameters such as reaction time, temperature, and concentration.

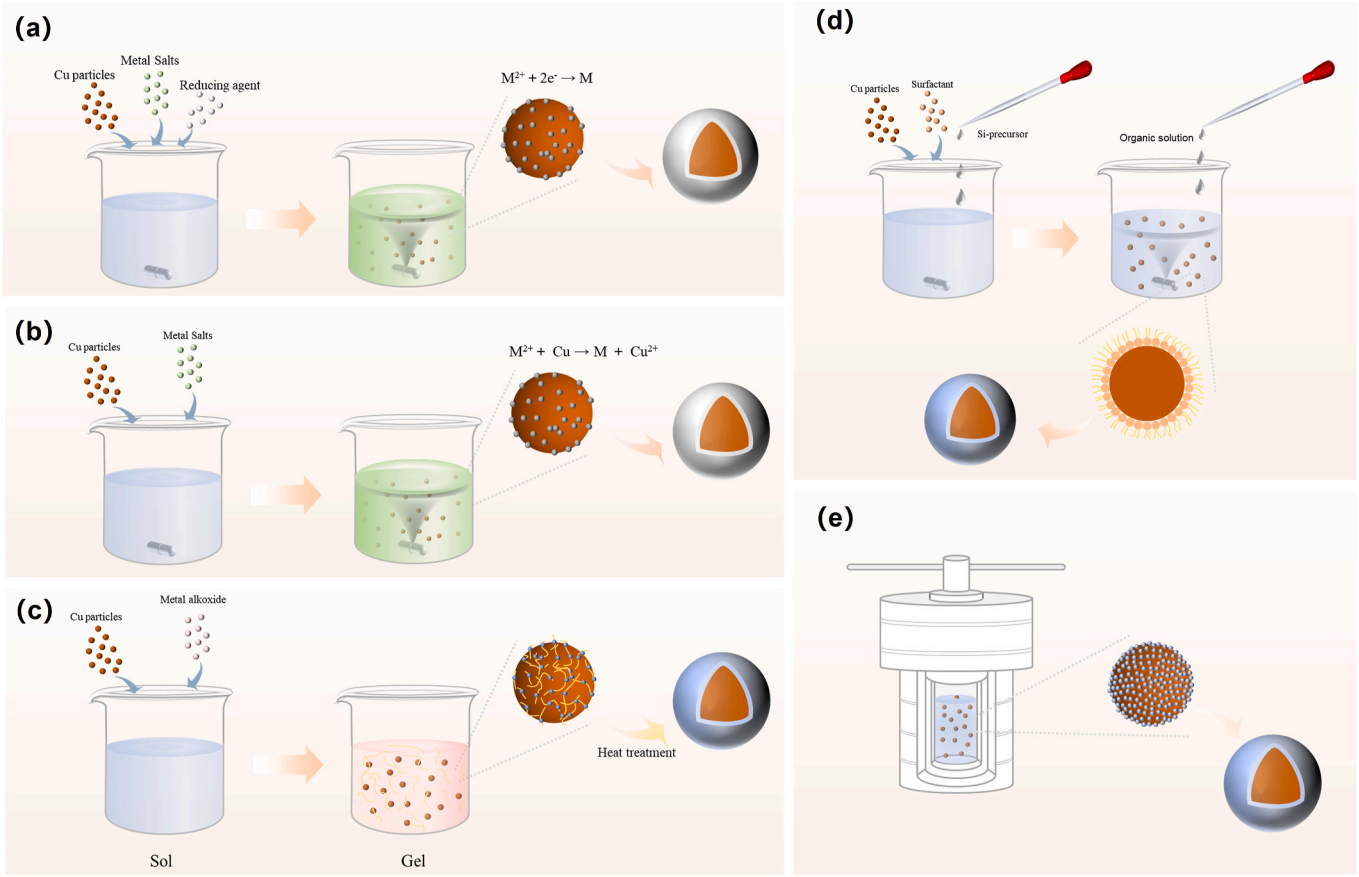

Fig. 7. Schematic diagram of the synthesis method of Cu-based core-shell structure. (a) Liquid phase reduction method. (b) Chemical plating method. (c) Sol-gel method. (d) Reverse microemulsion method. (e) Hydrothermal method.

- *Chemical Plating*: This approach relies on an autocatalytic reaction in an electroless environment to reduce metal ions, forming a dense and uniform shell around the copper core [78–80], as shown in Fig. 7b. By tuning variables such as temperature, pH, and reaction duration, the shell thickness is finely controlled, providing excellent versatility for customized applications.

2.2.1.2. Non-metal coating. For non-metal coatings, commonly employed methods include the sol-gel method, reverse microemulsion method, and hydrothermal method:

- *Sol-Gel Method*: This method involves transforming a metal oxide precursor into a gel through hydrolysis and polycondensation reactions, resulting in the formation of a non-metallic shell around the copper core [81], as shown in Fig. 7c. It is particularly effective for producing high-precision, uniform coatings.
- *Reverse Microemulsion Method*: Employing surfactants, this method creates a controlled microenvironment consisting of oil and water phases, as shown in Fig. 7d. The confined environment facilitates the hydrolysis and polycondensation of silicon precursors, enabling the formation of a uniform shell around the copper core [82].
- *Hydrothermal Method*: Conducted under high-temperature and high-pressure conditions, this method produces high-quality non-metallic shells with crystalline structures around copper cores, as shown in Fig. 7e. The approach is known for its rapid reaction rates and product quality [83–85].

Through continuous development and optimization of these synthesis methods, precise control over the dimensional, morphological, and compositional properties of Cu-based core-shell structures has been achieved to meet the stringent demands of high temperature and high reliability applications.

2.2.2. Research progress

Research on Cu-based core-shell structures has been developed during the past years. Early studies on low-temperature connection technologies showed that critical parameters in chip mounting materials include thermal stability, interface bonding, and long-term reliability. Early studies focused on low-melting-point shells, such as Sn, to enable low-temperature sintering. Li et al. [86] prepared Cu@Sn particles via electroplating, where the Sn shell reacted with the Cu core to form high-melting-point Cu-Sn IMCs. Reflow at 250 °C produced shear strengths of 29.35 MPa and 18.78 MPa after aging at 400 °C and 500 °C, respectively (Fig. 8a).

To enhance the mechanical strength and stability of Cu@Sn sintered materials, Chen et al. [27] incorporated SAC305 into the Cu@Sn

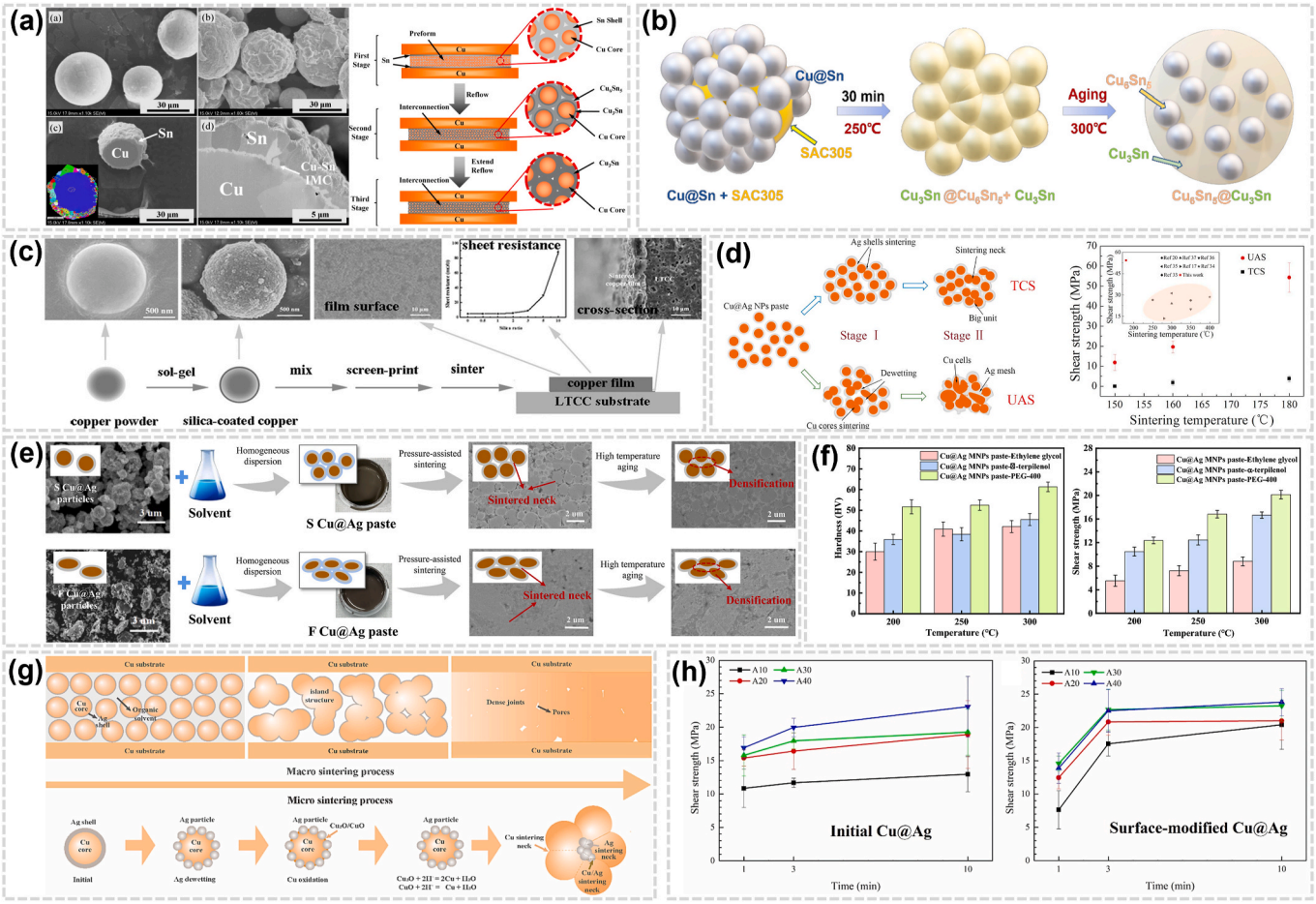

Fig. 8. Research progress of Cu-based core-shell structure sintering pastes. (a) The morphology of Cu particles before and after electroless tin plating and the microstructure of Cu@Sn core-shell structure [86]. (b) Schematic diagram of Cu@Sn with SAC at 250 °C reflux and 300 °C aging [27]. (c) Schematic diagram of silica-coated copper powder with different silica contents prepared by the sol-gel method, sheet resistance, and microstructure [87]. (d) Schematic representation of the microstructural evolution of sintered joints obtained by ultrasonic-assisted sintering (UAS) and hot pressing sintering (TCS), and the variation of shear strength with temperature, with insets showing comparison with recent reports in this field [26]. (e) The sintering evolution of Cu@Ag pastes [91]. (f) Hardness and shear strength of Cu@Ag MNPs paste sintered with ethylene glycol, α-terpineol, and PEG-400 at different sintering temperatures for 20 min [92]. (g) Macro and Micro sintering mechanism of Cu@Ag nano paste [93]. (h) Shear strength of bondlines containing initial and surface-modified submicron Cu@Ag particles with different Ag content after sintering at 250 °C with N_2 blowing as a function of bonding time [94].

structure, achieving shear strengths exceeding 60 MPa after aging at 300 °C for 800 h (Fig. 8b). The Sn shell protected the Cu core from oxidation and CuO loss during reflow. However, Sn's susceptibility to oxidation and corrosion in humid or corrosive environments compromised the long-term reliability of the joints.

To address these limitations, researchers explored coatings with superior chemical stability, high-temperature endurance, and corrosion resistance, such as silicon dioxide (SiO_2) and nickel (Ni). Yang et al. [87] employed the sol-gel method to synthesize silica-coated copper powders, achieving excellent bonding properties and chemical stability (Fig. 8c). However, silica's poor thermal and electrical conductivity limited overall performance. Choi et al. [88] reported Cu@Ni core-shell nanoparticles that retained high electrical conductivity and stability under extreme conditions of temperature and humidity. Although it improves oxidation resistance, nickel's thermal (~90 W/mK) and electrical conductivity (~14.3×10^6 S m^{-1}) are far lower than those of copper (~400 W/mK). Therefore, the formation of intermetallic compounds between nickel and copper at elevated temperatures may result in joint embrittlement and diminished reliability.

Building on the success of commercially applied low-temperature sintering silver paste, current research has turned to Cu@Ag core-shell structures for enhanced thermal/electrical conductivity, reliability, and cost-effectiveness. Ji et al. [26] reported shear strengths of 54.27 MPa at temperatures as low as 160 °C using ultrasonic-assisted sintering (Fig. 8d). Similarly, Lee et al. [89] explored rapid sintering of Cu@Ag particles in air, achieving shear strengths of 20~24 MPa at 350 °C under pressures of 5~10 MPa. To improve sintered layer density and conductivity, dual-sized nano/micro-Cu@Ag pastes demonstrated shear strengths exceeding 20 MPa under low-temperature rapid sintering conditions. While strides have been made in material synthesis and performance, a deeper understanding of the sintering mechanisms for new materials like Cu@Ag is still in its infancy. Wang et al. [90] employed finite element simulations to model Cu@Ag sintering, establishing a mathematical relationship between porosity, thermal conductivity, and sintering parameters. Experimental validation with Cu@Ag pastes confirmed the accuracy of the model, offering insights into sintering mechanisms. Further research of Cu@Ag sintering materials by Chen et al. [91] and Zhou et al. [92] examined the influence of organic solvents on Cu@Ag paste properties. Chen's analysis has not only focused on the influence of material structure on performance, but also on how organic solvents used during the paste preparation affect the final outcomes, as shown in Fig. 8e. Zhou's analysis of three solvents (Fig. 8f), including ethylene glycol, pinacol, and PEG-400, revealed that PEG-400, with its optimal boiling point and viscosity, produced superior sintered films, achieving a resistivity of 43.82 μΩ cm, a hardness of 61.3 HV, and shear strength of 20.14 MPa. Additionally, flake-shaped Cu@Ag particles synthesized using a pine alcohol-PEG formulation exhibited denser microstructures. These samples achieved a shear strength of 36.15 MPa, which is approximately 20 % higher than that of spherical particles. Moreover, they demonstrated enhanced creep resistance under high-temperature conditions.

Recent research has addressed the dewetting behavior of silver layers of Cu@Ag particles, which exposes internal copper to oxidation, reducing joint strength. Wen et al. [93] used nanoscale Cu@Ag pastes with low-boiling-point solvents, achieving fully dense sintered joints at 300 °C. Despite its effectiveness, the complexity and cost of nanoparticle synthesis remain challenges (Fig. 8g). Lee et al. [94] introduced a surface modification approach using stearic acid to suppress silver dewetting, achieving shear strengths of 17.56 MPa at 250 °C under 10 MPa pressure, a significant improvement over unmodified joints (11.67 MPa), as shown in Fig. 8h. Additionally, air thermogravimetric testing confirmed the efficacy of this surface modification in preventing internal copper oxidation and suppressing silver dewetting.

To further enhance sintering performance, researchers are now exploring multi-layer coatings such as Cu@Sn@Ag [95] and Cu@In@Ag [96]. These structures addressed single-layer limitations by providing improved mechanical strength, thermal conductivity, and environmental stability, paving the way for advanced applications in high-performance electronic packaging.

In addition to conventional metal shell structures, recent studies have demonstrated that organic molecular coatings can also provide effective oxidation resistance. For example, imidazole-based compounds have been shown to form robust surface layers on copper nanoparticles, significantly enhancing their antioxidant capacity and storage stability without compromising sinterability. These organic-coated Cu particles can serve as low-cost, environmentally friendly alternatives to Ag- or Sn-coated systems, especially in applications requiring long-term shelf life and simplified processing conditions [97,98].

The sintering performance of representative Cu-based core-shell structures is summarized in Table 3, highlighting that pressure-assisted sintering remains the dominant method. Innovative techniques, including ultrasonic-assisted and laser pulse sintering, have also emerged, demonstrating exceptional shear strength, conductivity, and reliability.

2.3. Cu-based alloy composite materials

Copper core-shell structures have improved copper's stability in atmospheric conditions and mitigated its tendency for spontaneous oxidation. However, practical applications are still hindered by limitations in manufacturing processes and cost-effectiveness. Furthermore, repeated thermal cycling, which is common in power devices, causes a radial gradient in thermal stress distribution within core-shell structures, leading to performance degradation. To meet the strict requirements for uniform stress distribution in the sintered layer, Cu-based alloy composite sintering pastes have emerged as a promising alternative to address these challenges.

Currently, Cu-based alloy materials are primarily synthesized through liquid-phase reduction or dual-beam pulsed laser deposition [102]. Fig. 9 outlines the preparation principles and operational procedures for these two methods. The sintering properties of representative Cu-based alloy pastes are summarized in Table 4, with Ag–Cu and Sn–Cu alloys being the primary focus of current researches. Beyond the choice of alloy materials, ongoing studies emphasize optimizing sintering parameters such as temperature, pressure, atmosphere, and particle size.

Alloying strategies modify the properties of base metals while retaining the inherent benefits to gain better thermal and electrical conductivity, lower production costs, and higher resistance to electrochemical migration. Besides, introducing alloying elements enhances mechanical properties, corrosion resistance, and oxidation tolerance, enabling sintering at relatively lower temperatures. For example, Zhang et al. [103] pioneered the use of copper-silver alloy nanoparticles synthesized via glucose chemical reduction. The nanoparticles exhibited no detectable signs of oxidation during sintering in air. The resultant paste demonstrated excellent electrochemical migration resistance and mechanical properties, achieving a maximum shear strength of 35 MPa. Similarly, Liu et al. [104] developed a copper-silver composite nanoparticle paste for low-temperature bonding. At sintering temperatures of 225 °C and 250 °C, shear strengths of 18.9 MPa and 22.8 MPa were achieved, respectively (Fig. 10a).

However, the sintering temperature remained notably higher compared to pure silver pastes, posing challenges for low-temperature solidification. To address this issue, Zhou et al. [105] synthesized Ag–Cu alloy nanoparticles via polyol chemical reduction, which maintained oxidation resistance up to 350 °C in air. Notably, sintering at 160 °C resulted in a shear strength of 50 MPa (Fig. 10b), marking a step toward achieving low-temperature bonding. Copper-silver alloy materials are also promising in printed electronics applications, particularly for flexible and wearable devices where low-temperature sintering is required. Zhong et al. [106] developed compositionally controllable Cu–Ag nanoparticles and formulated stable nano-inks, enabling

Table 3
Summary of preparation methods and properties of Cu-based core-shell structures composite sintered materials.

Authors	Year	Materials	Processing	Porosity	Properties of the sintered joints					Ref.
					Shear Strength	Elastic Modulus	Hardness	Thermal Conductivity	Electrical Conductivity	
Li et al.	2016	**Cu@Sn** (20–30 μm)	250 °C, 20/40 min, 4 mm × 7 mm	/	29.35 MPa (400 °C); 18.78 MPa (500 °C)	/	/	/	/	[86]
Jung et al.	2020	**Cu@Sn** (2 and 7 μm)	300 °C, 15 MPa, 30 min, 3 mm × 3 mm	/	40 MPa (2 μm); 50 MPa (7 μm)	/	/	/	/	[99]
Chen et al.	2022	**Cu@Sn** (3–5 μm), SAC305	250 °C, 1 MPa, 30 min, 5 mm × 5 mm	/	46.7 MPa (25 °C); 63.2 MPa (300 °C)	/	/	/	/	[27]
Choi et al.	2018	**Cu@Ni** (56.3/146.8 nm)	Intense Pulsed Light Sintering, 0.25–3.41 J cm^{-2}	/	/	/	/	/	52 μΩ cm	[88]
Yang et al.	2017	**Cu@SiO_2** (1.5–3 μm)	910 °C, N_2, 60 min, 9 mm × 9 mm	/	/	/	/	/	6 mΩ cm	[87]
Wu et al.	2023	**Cu@Cu(I)** (50/80/150/200 nm)	250 °C, 50/50/120/120 s, 5 mm × 5 mm	/	/	/	/	/	4.5/4.5/5.55/11.1 mΩ cm	[74]
Ji et al.	2018	**Cu@Ag** (70 nm)	150/160180 °C, 0.2 MPa, 35 kHz, 10 s, 230 W	/	11.9/20.0/54.3 MPa	/	/	/	/	[26]
Kim et al.	2021	**Cu@Ag** (1.6–1.7 μm)	Intense Pulsed Light Sintering, 9–13 J cm^{-2}	/	/	/	/	/	15.18 μΩ cm	[100]
Lee et al.	2022	**Cu@Ag** (1.5 μm/200 nm)	300 °C, 5 MPa, 10 min, 3 mm × 3 mm	/	45 MPa	/	/	/	/	[89]
Zhou et al.	2023	**Cu@Ag** (1.5 μm/200 nm)	200/250/300 °C, 20 min	/	12.36 MPa, (200 °C); 16.83 MPa (250 °C); 20.14 MPa (300 °C)	8.1 GPa	61.3 HV	/	43.82 μΩ cm	[92]
Chen et al.	2023	**S Cu@Ag** (1–2 μm)/ **F Cu@Ag** (1–2 μm)	250 °C, 20 MPa, 600 s, N_2, 2 mm × 2 mm	/	30.31/36.15 MPa	53/59 GPa	0.65/1.75 GPa	/	/	[91]
Won et al.	2023	**Cu@Ag** (1.1 μm)	250 °C, 9 MPa, N_2, 3 mm × 3 mm	/	16.9 MPa	/	/	/	/	[101]
Wen et al.	2024	**Cu@Ag** (30 nm)	180/200/250/300 °C, 10 MPa, 5/10/30/60 min, 5 mm × 5 mm	/	<5/10/17.3 MPa	/	/	/	/	[93]
Lee et al.	2024	**Cu@Ag** (1.1 μm)	250 °C, 10 MPa, 10 min, 3 mm × 3 mm	/	20.41 MPa	/	/	/	/	[94]
Zhang et al.	2023	**Cu@Imidazole-Compound** (200–600 nm)	300 °C, 2 MPa, 30 min, Ar–H_2, 4 mm × 4 mm	/	20~32.5 MPa	/	/	/	4.86–14.7 μΩ cm	[97]

room-temperature sintering on paper substrates. This advancement supports the development of flexible printed electronics and room-temperature sintering technologies. Cu_3Sn IMCs offer superior oxidation resistance, higher melting points, and lower raw material costs compared to Ag, making copper-tin alloys highly attractive for research. Wang et al. [107] reported a copper-tin alloy paste capable of air sintering, producing joints with shear strengths comparable to those sintered under vacuum conditions. By employing dual-size metal particles, a bonding strength of 40 MPa was available, outperforming traditional Sn-based solder joints (19 MPa) and all-Cu_6Sn_5 joints (17.7 MPa), as shown in Fig. 10c. Despite the successful preparation of Cu_3Sn particles, the sintering temperature remained elevated at 300 °C. To address this challenge, Dimitrov et al. [108] developed polytin-coated nanoporous copper (np-Cu). This highly active material enabled the formation of dense Cu_3Sn alloy films at temperatures as low as 200 °C, suitable for low-temperature bonding.

In summary, the adoption of Cu-based alloy strategies represents an advancement in microelectronics packaging. Ongoing research focuses on optimizing synthesis methods for scalability and cost-effectiveness, further reducing sintering temperatures, and enhancing performance through controlled alloy composition and morphology. In particular, precise and customizable adjustments to the alloy structure are critical for meeting the diverse requirements of modern applications.

2.4. Further systematic overview

In the previous review, we systematically assessed the performance of various types of Cu-based sintered materials, including mechanically blended powders, core-shell structures, and alloyed systems. It was found that the final properties of these composites were collectively governed by multiple factors, such as filler composition and architecture, particle morphology, and sintering process parameters. Among the reported performance indicators, shear strength remains the most extensively studied metric, while data on thermal and electrical conductivity are relatively scarce, particularly for Cu-based core-shell and alloyed systems. In contrast, studies on modulus and hardness are even more limited, often exhibiting substantial variation depending on the testing methodology. For instance, Hou et al. [57] highlighted regional inconsistencies in nanoindentation results, underscoring the urgent need for standardized characterization protocols. To address these gaps, future research should prioritize the unification of mechanical and functional property evaluation standards, enabling a comprehensive and reliable comparison of Cu-based sintered joints across different composite systems.

To provide a comparative overview, the performance of Cu-based sintered pastes was further summarized under different composite strategies, using three widely adopted indicators including shear strength, thermal conductivity, and electrical conductivity, as illustrated in Fig. 11.

For metal particle mixtures, core-shell structures, and alloyed pastes,

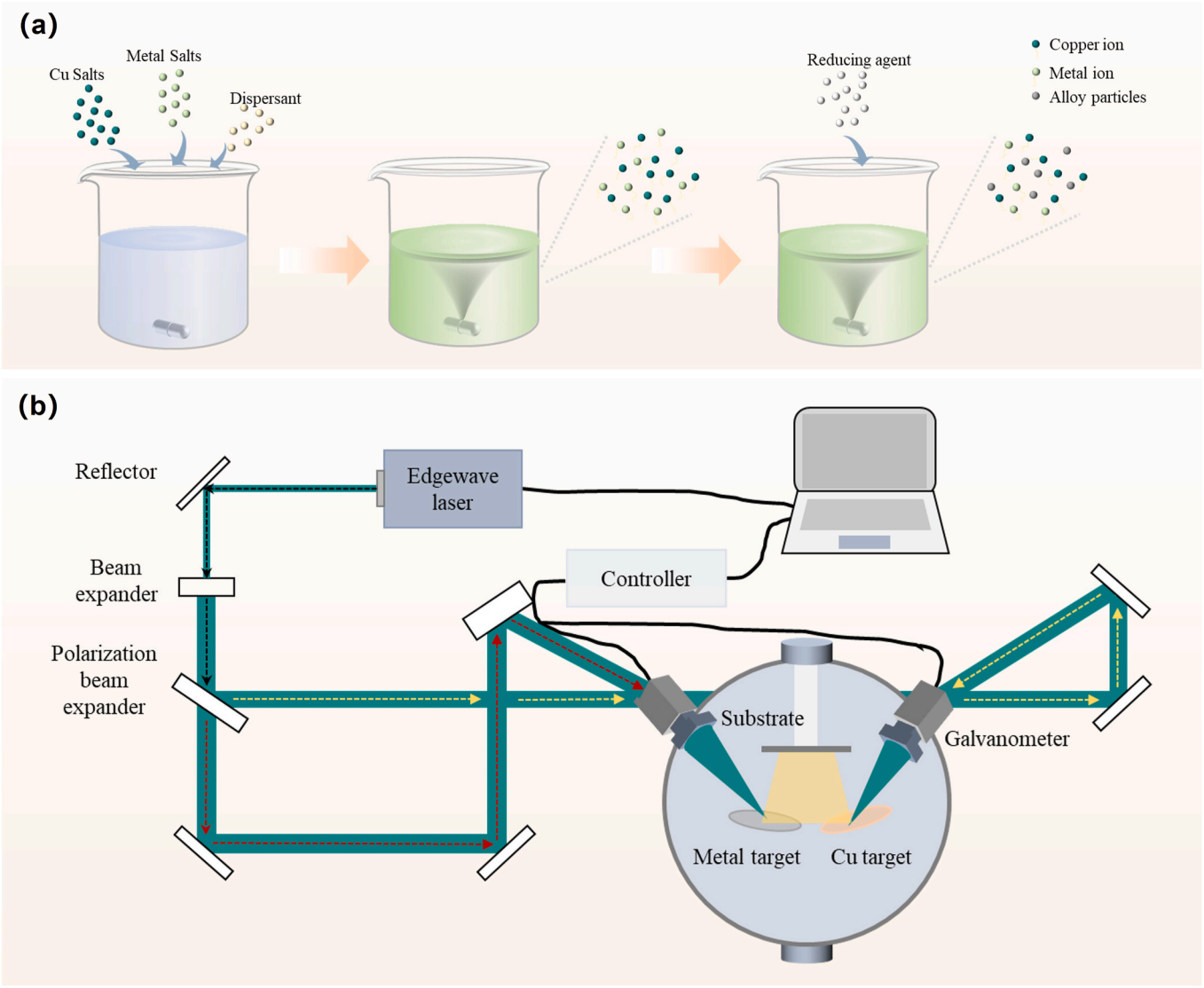

Fig. 9. Schematic diagram of Cu-based alloy material synthesis: (a) Liquid phase reduction and (b) dual-beam pulsed laser deposition method.

Table 4
Summary of preparation methods and properties of Cu-based alloy composite sintered materials.

Authors	Year	Materials	Processing	Porosity	Properties of the sintered joints					Ref.
					Shear Strength	Elastic Modulus	Hardness	Thermal Conductivity	Electrical Conductivity	
Zhang et al.	2015	**Ag–Cu** (20–50 nm)	180/200/250/300/350 °C, 100 min, 2 MPa, discs with diameters of 6 mm and 10 mm, and a height of 5 mm	/	33 MPa (300 °C)	/	/	/	/	[103]
Liu et al.	2019	**Ag–Cu** (9 nm)	175/200/225/250 °C, 5 MPa, 30 min, Ar	/	18.9 MPa (225 °C); 22.8 MPa (250 °C)	/	/	/	/	[104]
Zhou et al.	2019	**Ag–Cu** (60 nm)	160 °C	/	50 MPa	/	/	/	/	[105]
Guo et al.	2024	**Ag–Cu** (100–300 nm)	300 °C, 20 MPa, 30 min, Formic acid	10.8 %	/	/	/	/	/	[102]
Wang et al.	2022	**Sn–Cu** (55/120 nm)	260/280/300/320 °C, 10 MPa, 10 min, 5 mm × 5 mm	/	40.4 MPa	/	/	/	29.1 μΩ cm	[107]

the intrinsic high conductivity of metallic constituents ensures superior thermal and electrical performance. In contrast, non-metallic fillers are primarily introduced to lower the activation energy for copper particle bonding, thereby promoting densification at reduced temperatures. These fillers also enhance the mechanical robustness and creep resistance of the sintered layer.

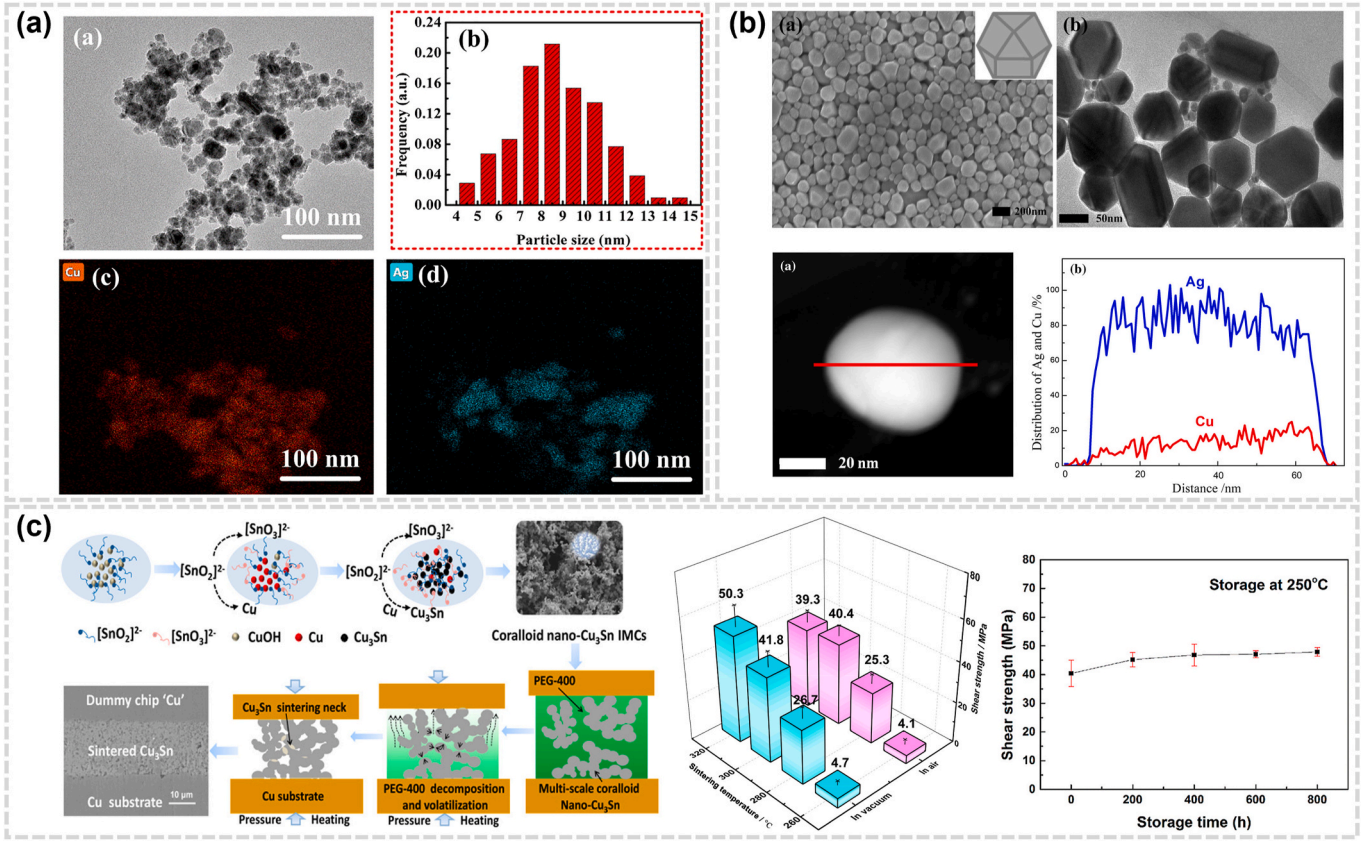

Fig. 10. Research progress of Cu-based alloy sintering pastes. (a) Morphology, size distribution and composition of Cu–Ag alloy nanoparticles [104]. (b) Morphology and element content distribution of Ag–Cu alloy nanoparticles [105]. (c) Schematic diagram of the synthesis and sintering process of coral-shaped nano Cu_3Sn, and comparison of shear strength and high-temperature aging resistance of joints sintered at different sintering atmosphere temperatures [107].

Among metallic additives, Sn and Ag are most commonly employed. Sn facilitates better wettability between Cu and the substrate or chip, and supports low-temperature sintering. However, its tendency to oxidize and form brittle interfacial phases through complex reactions can undermine interfacial strength. Ag, in comparison, offers superior oxidation resistance and thermal performance, while retaining the advantages of Sn, making it particularly suitable for applications with stringent requirements on heat dissipation, electrical performance, and reliability, such as power module packaging, RF devices, and high-temperature electronics. Metal oxides such as AgO, CuO, and Cu_2O also exhibit promising capabilities in improving thermal stability and mitigating oxidation in Cu pastes. Their incorporation has been shown to enhance the long-term thermal reliability of sintered joints, which is essential for electronic devices operating in harsh environments.

In addition, non-metallic fillers such as epoxy resin have demonstrated excellent adhesion and mechanical reinforcement, striking a favorable balance between structural strength and thermal performance. Carbon-based nanofillers, including carbon nanotubes (CNTs) and graphene, offer remarkable enhancements in hardness and thermal conductivity even at low loadings. These fillers provide tunable performance benefits, enabling compositional and structural tailoring of the composite to match specific application scenarios.

To further understand the origins of performance variation among Cu-based composite sintered materials, it is essential to examine the interplay between material design and processing parameters. As illustrated in Fig. 12, the overall performance of these materials is intricately influenced by multiple factors, including particle morphology, composite architecture, component ratios, and sintering conditions. Notably, composite pastes with multi-scale or hierarchical structures often undergo distinct sintering mechanisms, which in turn affect the formation of microstructures and ultimately determine joint integrity and thermal/electrical behavior. Among all processing variables, sintering temperature, pressure, and duration play particularly pivotal roles in controlling densification, interfacial bonding, and microstructural evolution. Proper optimization of these parameters has been shown to effectively reduce porosity, enhance hardness and elastic modulus, and improve both thermal and electrical conductivity, thereby enabling a more reliable and high-performance packaging solution.

Looking ahead, future research should emphasize multi-parameter optimization strategies to achieve balanced improvements across mechanical, thermal, and electrical domains. This includes the refinement of metallic particle structure and composition, the selection and proportioning of solvents and fillers, and the precise control of sintering conditions. Ultimately, these efforts will contribute to the development of high-performance Cu-based composite materials with enhanced reliability, tailored for next-generation electronic packaging applications.

3. Reliability analysis

Reliability is crucial for power electronic packaging applications. This section explores the reliability aspects of Cu-based sintered materials, focusing on high-temperature storage, thermal cycling, corrosion, and electrochemical migration. The discussion highlights key challenges and solutions to ensure the effective application of Cu-based sintered joints in electronic packaging under harsh conditions.

3.1. High-temperature storage test

The high-temperature storage (HTS) test is a vital reliability assessment for Cu-based sintered materials in power electronics, particularly for applications exposed to prolonged high-temperature conditions. Stability under sustained thermal stress is crucial for maintaining

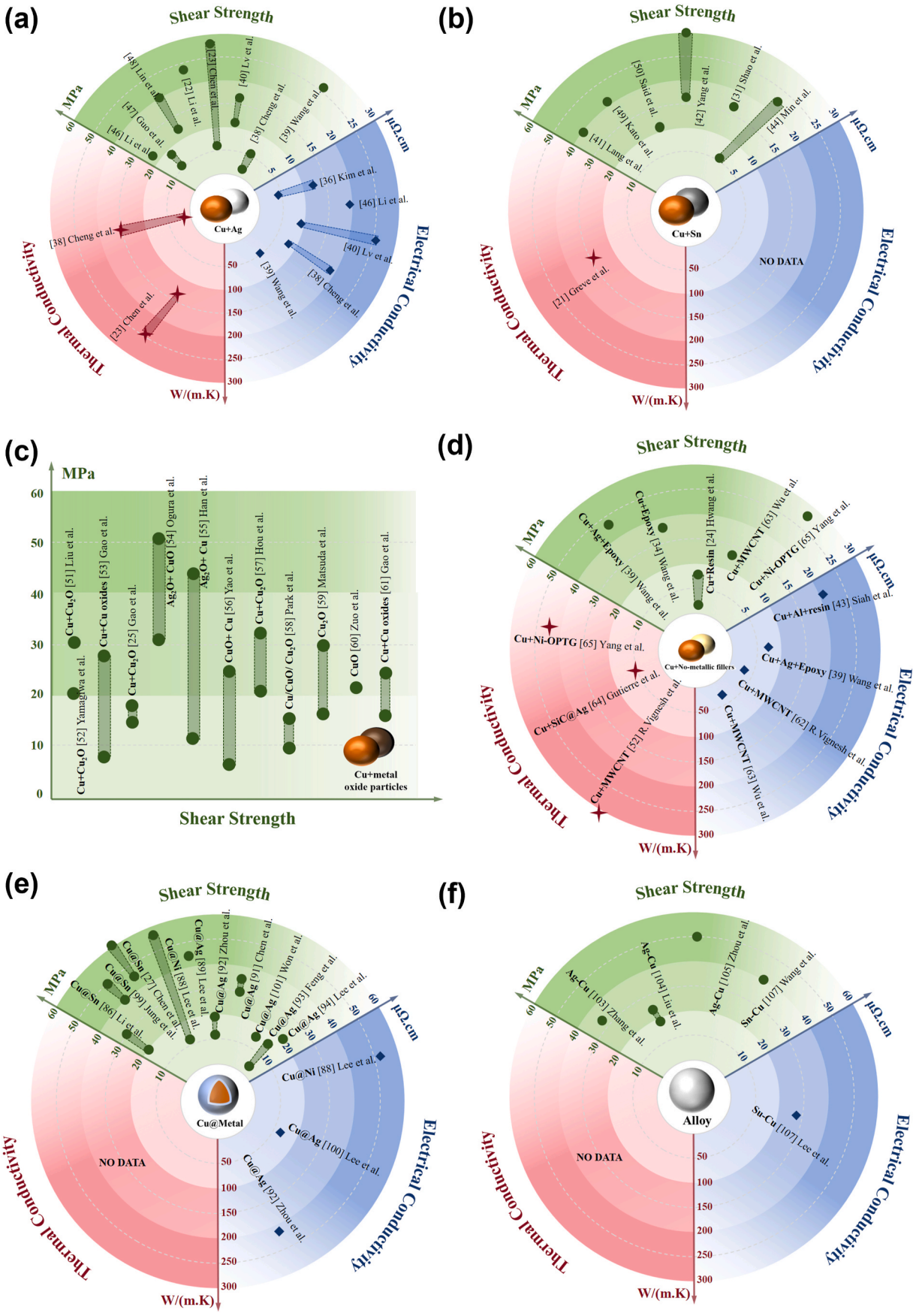

Fig. 11. Comparison of mechanical and thermoelectric properties of different copper-based composite sintered materials: (a) copper-silver blend; (b) copper-tin blend; (c) copper and oxide blend; (d) copper and non-metallic filler blend; (e) copper core-shell structure; (f) copper-based alloy.

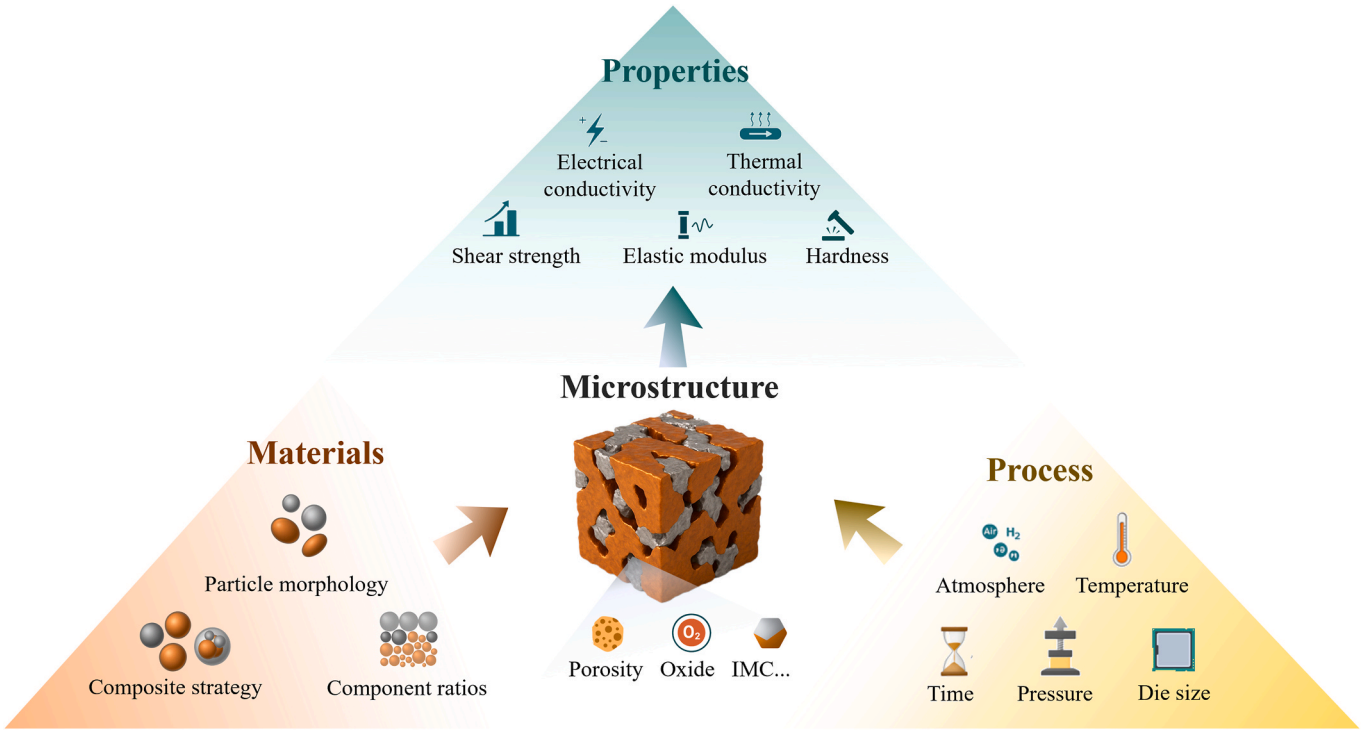

Fig. 12. Key factors that influence the properties of sintered materials.

performance and reliability in applications such as electric vehicles, power modules, and high-frequency devices. HTS testing evaluates the effects of thermal stress on mechanical properties, such as shear strength, and identifies potential failure mechanisms, including grain growth, oxidation, and phase transformations.

3.1.1. *Cu–Ag system*

Cu–Ag composites, including both blended and core-shell structures, demonstrated strong resistance to oxidation and relatively stable mechanical properties during HTS testing. The Cu–Ag blended joints exhibited an increase in shear strength from 51.7 MPa to approximately 82 MPa after 400 h at 250 °C in air [39]. This improvement was attributed to the presence of silver, which played a critical role in mitigating oxidation and improving bonding strength compared to pure copper joints. For Cu@Ag core-shell structures, the shear strength of Cu@Ag sintered joints increased from 30.3 MPa to around 62 MPa, suggesting that the silver shell provided an effective barrier against oxidation, thereby improving the mechanical integrity of the joints, as exhibited in Fig. 14a [91]. Both Cu–Ag blended and core-shell composites displayed significant potential for high-temperature applications due to their enhanced thermal properties and resistance to oxidation.

3.1.2. *Cu–Sn system*

Cu–Sn systems, including both blended and core-shell structures, showed complex behavior under HTS conditions due to the formation of IMCs. During HTS testing, the formation of IMCs such as Cu_6Sn_5 and Cu_3Sn was observed, which played a dual role. On one hand, these IMCs contributed to structural stability by reducing Kirkendall void formation, thereby enhancing shear strength retention over extended thermal exposure. For example, Cu–Sn composites sintered joints reported by Lang et al. initially had a shear strength of approximately 40 MPa, which increased to around 50 MPa after 1800 h at 300 °C in air, highlighting the potential for these IMCs to reinforce joint performance over extended periods [41]. On the other hand, excessive IMC growth can lead to mechanical degradation. Composite sintered joints fabricated using Cu and Sn-based alloys have shown a noticeable reduction in shear strength after prolonged HTS, particularly under moderate thermal conditions (e.g., 150 °C in air for 500 h), as shown in Fig. 14b [50]. Similarly, Cu–Sn core-shell structures presented a reduction in shear strength from 25.4 MPa to 20.14 MPa after storing Cu–Sn joints at 300 °C for 1200 h in air, attributing the reduction to excessive IMC growth and oxidation of the joint surface, as illustrated in Fig. 14c [27]. These findings underscore the importance of regulating IMC evolution to ensure the mechanical reliability of Cu–Sn sintered systems under high-temperature operating conditions, regardless of whether the microstructure follows a blended or core-shell configuration.

3.1.3. *Cu-oxide system*

Copper combined with oxide fillers demonstrated specific advantages and challenges under HTS conditions. For example, a pressureless Cu–Cu bonding was developed using preoxidized Cu microparticles sintered in a formic-acid atmosphere, leading to the formation of a Cu_2O layer on the Cu microparticles, which initially contributed to effective bonding by reducing interfacial voids and promoting a dense structure [53]. However, during prolonged thermal aging at 200 °C over 1000 h, the shear strength markedly decreased from approximately 27.5 MPa–~0 MPa, indicating severe oxidation and mechanical degradation, as exhibited in Fig. 14d. In another study, Cu_2O nanoparticles, along with PEG as a reducing agent, were used to improve the antioxidative performance of sintered Cu joints [59]. The presence of PEG played a role in reducing the Cu_2O and controlling the formation of the oxide layer, which contributed to maintaining mechanical strength during thermal aging at 250 °C for 1000 h, with shear strength increasing from approximately 35 MPa–50 MPa. This method effectively mitigated oxidation-induced degradation and enhanced the long-term stability of the Cu-oxide composites.

3.1.4. *Other systems*

Other Cu-based composites, including those incorporating epoxy and CNTs, have also been investigated for their performance under HTS conditions. The inclusion of CNTs in Cu-based sintered joints has proven beneficial for thermal stability. Cu-CNT joints maintained a shear

strength of 26.64 MPa after HTS at 250 °C for 168 h, with only a slight reduction to 25.14 MPa [63]. The CNTs provided reinforcement by inhibiting crack propagation and enhancing thermal conductivity, which mitigated thermal stress and degradation, thereby improving the stability of the sintered joints under prolonged high-temperature exposure. The CNTs provided structural reinforcement, mitigating the degradation associated with prolonged high-temperature exposure and enhancing the mechanical stability of the sintered joints. Epoxy-based copper composites were also studied for their HTS performance. A reduction in shear strength from 12.1 MPa to 10.46 MPa was observed after HTS at 175 °C for 72 h in air [24]. The epoxy served as an effective oxidation barrier, protecting the copper fillers and providing a certain degree of joint stability. Further investigations demonstrated that the incorporation of epoxy resin into Cu–Ag sintered joints could effectively enhance their HTS reliability. Specifically, the Cu–Ag-epoxy composite maintained a relatively high shear strength of 48.54 MPa, which increased to approximately 95 MPa after 400 h at 250 °C in air [39]. This improvement is attributed to the epoxy resin functioning as a pore-filling agent, thereby reducing oxidation and enhancing joint stability, as illustrated in Fig. 14e. Nevertheless, the limited thermal stability of epoxy materials constrains their use in extremely high-temperature environments.

The summarized results from these studies, as shown in Fig. 13 and Table 5, highlight the effects of different fillers, sintering processes, and HTS testing conditions on the long-term high-temperature stability performance of copper-based composite sintered joints. Composite sintered materials prepared from Cu–Ag direct blending and Cu@Ag core-shell particles have shown considerable promise for high-temperature applications due to their excellent oxidation resistance and retention of mechanical properties. Meanwhile, Cu–Sn systems, especially those with optimized IMC formation, also displayed good performance. Cu and oxide systems, such as joint samples involving Cu_2O, showed potential for enhanced bonding and antioxidative stability, while challenges remained regarding prolonged exposure to HTS. Composites involving epoxy and CNTs provided additional reinforcement, though the application of epoxy was limited by the thermal stability. Future research should focus on optimizing filler composition, sintering parameters, and protective strategies to further improve the high-temperature reliability of these materials for power electronic packaging applications. Specifically, strategies such as oxidation-resistant coatings, encapsulants, and optimized sintering parameters, including temperature ramping rates and pressure adjustments, have shown potential in the reviewed literature. These approaches effectively minimize void formation, regulate IMCs' growth, and enhance bonding stability, thereby improving device performance under high-temperature conditions.

3.2. Thermal cycling test

Thermal cycling is a critical reliability test that assesses the durability of Cu-based composite sintered materials under fluctuating temperature conditions, particularly relevant for electronic applications exposed to harsh thermal environments. Thermal cycling leads to the development of thermal stress, primarily due to the mismatch in the CTE between different materials. Such phenomena may result in delamination, microcracking, and mechanical failure in sintered joints.

The results of thermal cycling tests from various studies illustrate the differences in reliability performance across different Cu-based sintered materials, as summarized in Fig. 15 and Table 6. For instance, Cu–Ag sintered joints have shown strong retention of shear strength after 450 cycles between −55 °C and 150 °C, maintaining an average shear strength of 25 MPa with minimal variation throughout the cycling

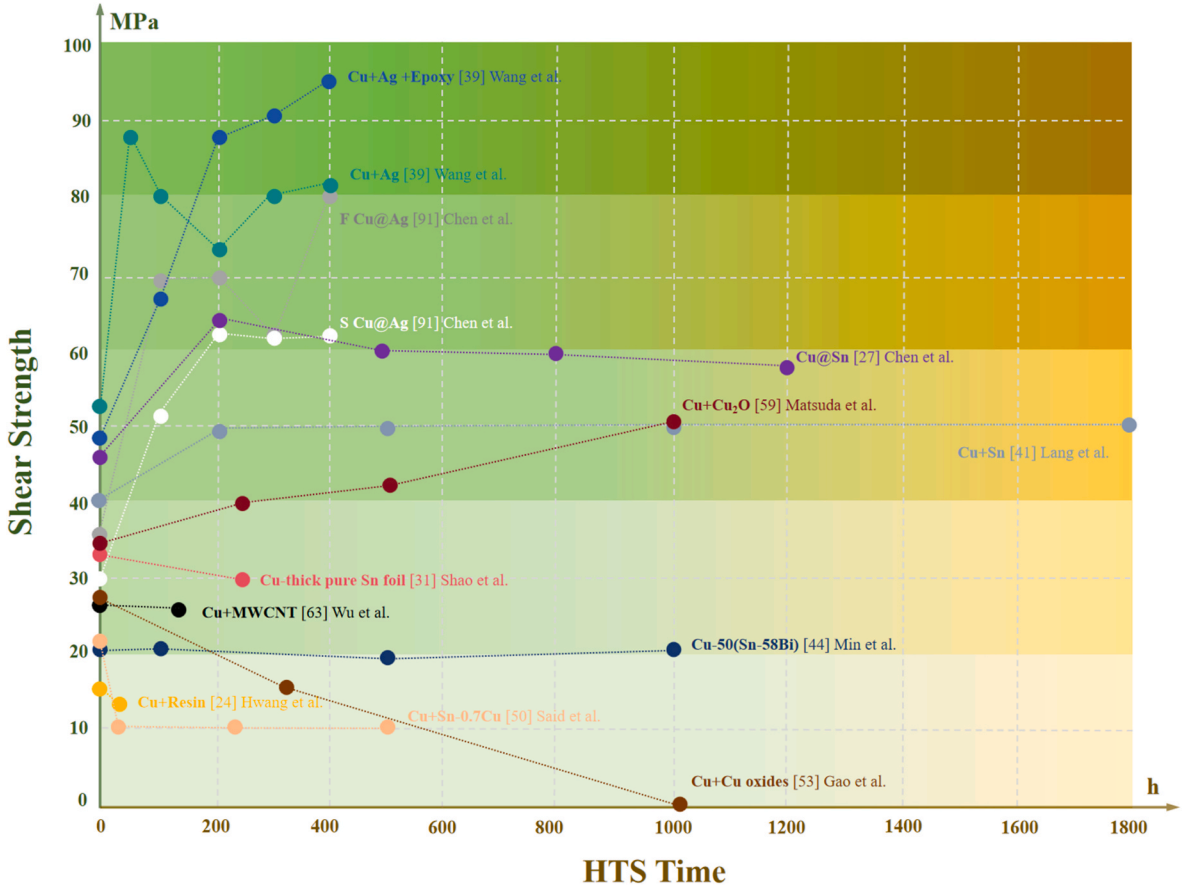

Fig. 13. Summary of shear strength changes of Cu-based composite sintered joints after HTS tests.

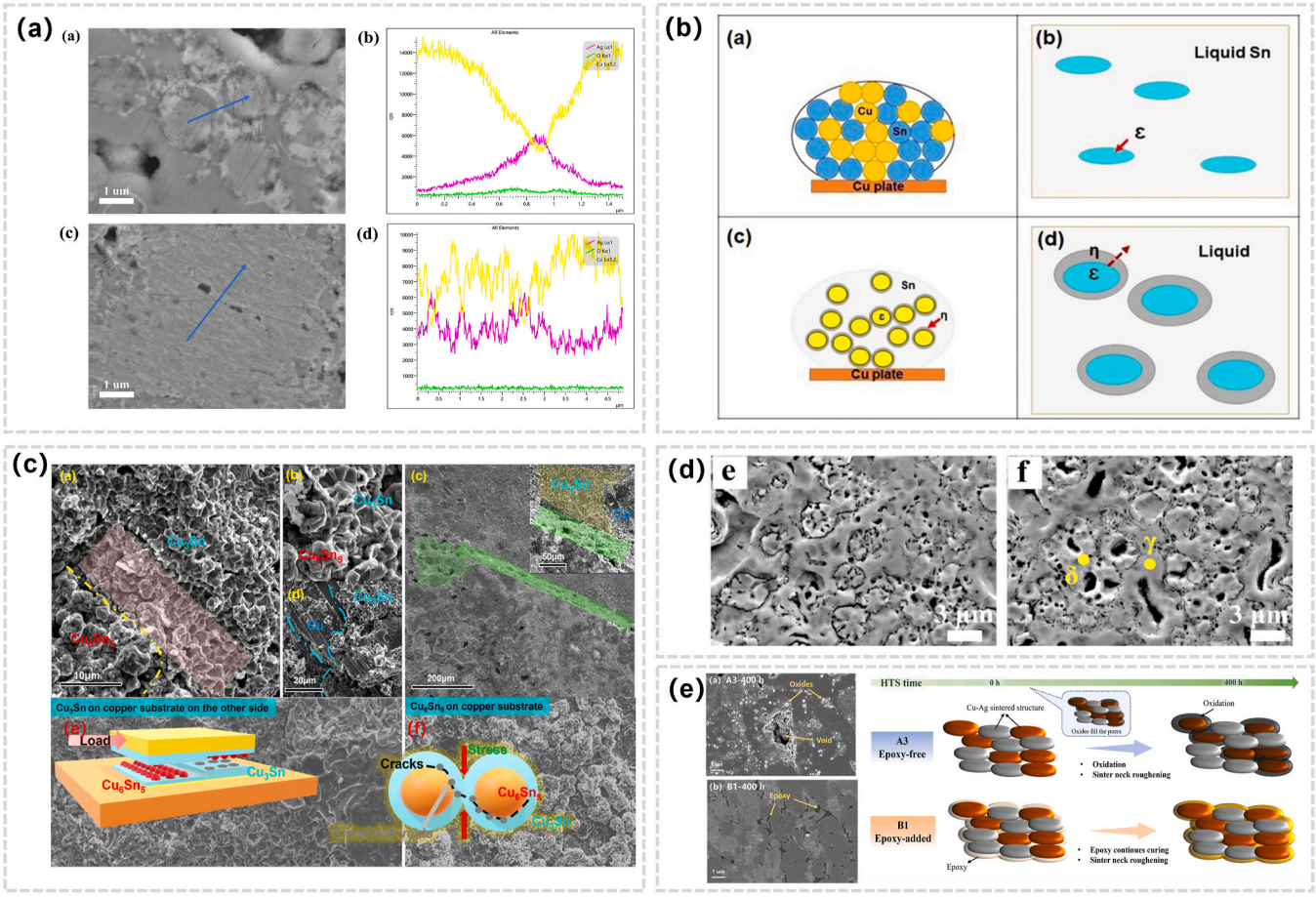

Fig. 14. (a) SCu@Ag and FCu@Ag SEM images and EDS mapping of sintered joints after 400 h aging [91];(b) Schematic diagram of TLPS SC10 solder paste on Cu substrate during soldering, liquid Sn (liquid phase) difuse into the Cu particles (solid phase) forming another solid phase (ε), the formation of another Cu6Sn5 intermetallic phase and d the ε phase needed to reach to the liquid Sn for the reaction to continue [50];(c) SEM images (SED) of shear fracture surface for the Cu@Sn sample aging 1200 h at 300 °C [27];(d) Cross-sectional SEM images of Cu–Cu bonding specimens after 72 h of aging, and 336 h of aging [53];(e) Local SEM photos and schematic diagram of the aging mechanism of the Cu–Ag joints section after 400 h HST, fabricated with and without epoxy [39].

process [39]. This reliability has been attributed to the incorporation of epoxy resin, which helps fill microvoids and mitigate oxidation effects during thermal cycling. In another case, Cu–Sn die-attach materials used in SiC power modules demonstrated stable performance after 1000 thermal cycles between −40 °C and 250 °C, with the average shear strength remaining around 40 MPa [49]. These results emphasize the high reliability of Cu–Sn TLPS pastes in maintaining joint integrity under extreme temperature variations. By contrast, Cu–Cu bonding based on preoxidized Cu microparticles showed some degradation in shear strength after cycling between −40 °C and 200 °C, despite similar microstructural features before and after testing [53]. This reduction in performance was primarily caused by the mismatch in the CTE between Cu and the Cu_2O phase formed during processing. The brittle nature of Cu_2O created crack initiation sites, which contributed to mechanical degradation during thermal cycling, as illustrated in Fig. 16a and b. Among the compared systems, Cu–Sn TLPS joints exhibited higher reliability under thermal cycling compared to Cu–Cu joints, which were prone to oxidation-related failure. Meanwhile, Cu–Ag composites demonstrated excellent resilience, aided by epoxy additives that helped suppress oxidation and minimize porosity-related mechanical degradation.

These findings collectively highlight the importance of material selection, microstructure optimization, and the incorporation of additives in enhancing the thermal cycling reliability of sintered Cu-based materials used in power electronics. By understanding the failure modes and addressing the challenges posed by CTE mismatches, meaningful improvements in the long-term reliability of these materials can be realized.

3.3. Corrosion test

With the ongoing development of marine resources, new energy applications such as offshore wind power, photovoltaics, and salinity-gradient power generation impose increasingly stringent requirements on-chip interconnect materials. Under complex service environments characterized by high humidity, high salinity, and corrosive substances, the corrosion-induced degradation of metal interconnect layers is greatly accelerated, leading to irreversible damage to device performance and reliability. Therefore, investigating and enhancing the service performance of chip interconnect materials in such harsh conditions is crucial for ensuring the reliability of power devices.

Early studies on the corrosion behavior of sintered materials in high-humidity and high-salinity environments have shown that material porosity plays a critical role in corrosion processes. For example, Kolbinger et al. [109] conducted electrochemical measurements to explore the relationship between the porosity of sintered silver and its corrosion behavior in artificial seawater. The results indicated that the open-pore structure had a pronounced impact on corrosion behavior, allowing the electrolyte to penetrate deeper, thereby initiating corrosion processes within the material, as shown in Fig. 17a. Reducing porosity was found to effectively decrease corrosion affinity and mitigate the depth of corrosion. Further research into the mechanical behavior of sintered

Table 5
Summary of HTS tests results of Cu-based composite sintered materials.

Authors	Year	Materials	HTS Processing	Shear Strength (MPa)		Ref.
				Initial	End	
Chen et al.	2023	**S Cu@Ag** (1–2 μm)	250 °C, air, 400 h	30.3	~62	[91]
Chen et al.	2023	**F Cu@Ag** (1–2 μm)	250 °C, air, 400 h	36.2	~80	[91]
Min et al.	2021	**Cu** (4 μm) + **Sn–58Bi** (35 μm) (Cu-50 (Sn–58Bi))	200 °C, air, 1000 h	10.36	~10	[44]
Wang et al.	2024	**F Cu** (1–3 μm) + **F Ag** (1–3 μm), content: Cu:Ag = 1:1	250 °C, air, 400 h	51.7	~82	[39]
Wang et al.	2024	**F Cu** (1–3 μm) + **F Ag** (1–3 μm) + **epoxy resin** (5 wt%), content: Cu:Ag = 1:1	250 °C, air, 400 h	48.54	~95	[39]
Wu et al.	2022	**S Cu** (20–60 nm, 0.2–0.6 μm and 1–2 μm) + **MWCNTs** (content: 0.6 wt%)	250 °C, air, 168 h	26.64	25.14	[63]
Hwang et al.	2021	**S Cu** (4 μm) + **F Cu** (20 μm) + **resin** (5, 10, 15 wt%), content: S Cu:F Cu = 1:1	175 °C, air, 72 h	2.81/ 12.1/ 16.23	2.12/ 10.46/ 12.98	[24]
Lang et al.	2013	**Cu** + **Sn**,<15 μm, content: Cu:Sn = 6:4	300 °C, air, 1800 h	~40	~50	[41]
Said et al.	2020	**F Cu** + **Sn-0.7 Cu** (45 μm) content: Cu = 10 wt%	150 °C, air, 500 h	20.19	~10	[50]
Shao et al.	2018	**Cu** (2 μm/20 μm)+20 μm-thick pure **Sn** foil	350 °C, air, 240 h	33.1	29.7	[31]
Chen et al.	2022	**Cu@Sn** (3–5 μm), SAC305	300 °C, air, 1200 h	46.7 (25 °C), 63.2 (300 °C)	~58	[27]
Gao et al.	2020	**Cu** particles, **Cu oxide** fragments, **Cu oxide** nanoparticles; Formic acid as reducing solvent	200 °C, air, 1008 h	~27.5	~0	[53]
Matsuda et al.	2023	**Cu_2O** nanoparticles; PEG 400 as reducing solvent	250 °C, air, 1000 h	~35	~50	[59]

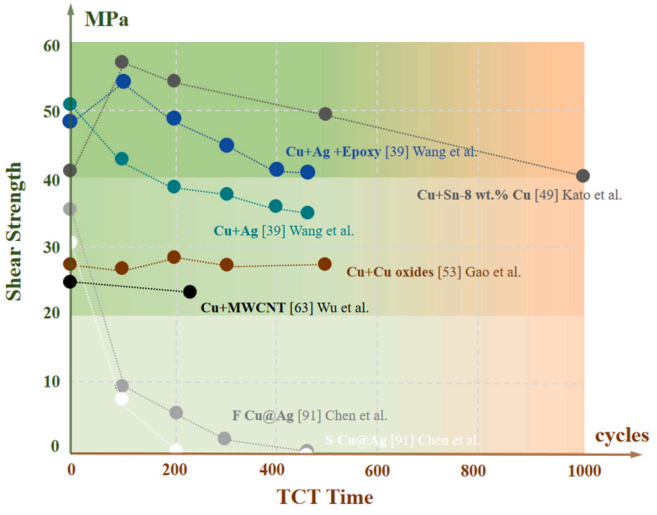

Fig. 15. Summary of shear strength changes of Cu-based composite sintered joints after HTS tests.

silver joints with varying porosity after seawater exposure revealed that corrosion filled the sintered pores with silver chloride, thereby increasing Young's modulus and indentation hardness in high-porosity samples, as shown in Fig. 17b. However, despite these improvements in mechanical properties, corrosion also created crack-prone areas along the edges of the sintered silver layer, compromising overall structural stability and reliability [110]. Similar relationships between porosity and corrosion behavior were also observed in sintered copper. Kotadia et al. [111] found that copper sintered at higher densities (i.e., lower porosity) exhibited better corrosion resistance in saltwater environments. Compared with pure copper and pure silver joints, Cu–Ag composite joints represent a compromise strategy that capitalizes on the advantages of both metals. Nevertheless, the potential difference between copper and silver can lead to galvanic corrosion, especially under humid conditions, thereby resulting in rapid device failure. To address this issue, Liu et al. [112] developed a thermodynamic–kinetic model to predict galvanic corrosion processes in Cu–Ag composite sintered materials, which they validated through in-situ electrochemical measurements in simulated seawater using different Cu–Ag particle sizes and solvent systems. Besides Cu–Ag sintered materials, other copper-based composite sintered materials encounter similar issues. Jung et al. [44] studied traditional intermetallic compound junctions in saltwater environments. They found that the Sn phase could not withstand salt spray conditions, resulting in the formation of compounds such as $Sn_3O(OH)_2Cl_2$. Moreover, interactions between residual Sn and Cu at high temperatures led to the formation of Kirkendall voids, which further reduced joint reliability. TLP with Cu and Sn-58 wt% Bi was reported to mitigate these issues. Salt spray tests in 5 % NaCl at 35 °C for 24, 48, and 96 h showed that forming Cu_3Sn intermetallic compounds enhanced corrosion resistance, thereby improving electrochemical and thermal bonding reliability.

In addition to high-salinity environments, corrosive gases such as sulfides pose challenges to chip interconnect materials. Fan et al. [113] conducted a comprehensive study on sintered copper samples to evaluate their behavior under sulfur-containing corrosive conditions, such as those found in offshore environments. For sintered copper samples, loose corrosion products were observed under elemental sulfur exposure, whereas densely layered corrosion products formed in an H_2S atmosphere. Corrosion induced by elemental sulfur was more severe, resulting in deeper penetration and marked reductions in elastic modulus and hardness, as shown in Fig. 17c. Furthermore, Liu et al. [34] examined four groups of sintered joints fabricated using different solvent systems under high-humidity H_2S conditions, revealing their respective sulfur corrosion mechanisms, as shown in Fig. 17d. The results indicated that sintered copper joints exhibited superior anti-corrosion behavior compared to sintered silver, especially when epoxy resin was added. However, thermal shock tests revealed a notable decline in the shear strength of corroded copper joints, highlighting the need for further optimization.

The current study highlights the major challenges faced by chip interconnection materials in harsh environments, such as high salinity, humidity, and corrosive gases. Understanding the intrinsic corrosion mechanisms of these materials is crucial for enhancing their corrosion resistance and service reliability. Although existing research has primarily concentrated on Sn-based, pure silver, and pure copper sintered

Table 6
Summary of TCT test results of Cu-based composite sintered materials.

Authors	Year	Materials	TCT Processing	Shear Strength (MPa)		Ref.
				Initial	End	
Chen et al.	2023	**S Cu@Ag** (1–2 μm)/**F Cu@Ag** (1–2 μm)	−55~150 °C, 2 cycles/h, 450 cycles	30.3/36.2	0	[91]
Wang et al.	2024	**F Cu** (1–3 μm) + **F Ag** (1–3 μm), content: Cu:Ag = 1:1	−55~150 °C, 2 cycles/h, 450 cycles	51.7	34	[39]
Wang et al.	2024	**F Cu** (1–3 μm) + **F Ag** (1–3 μm) + **epoxy resin** (5–10 wt%), content: Cu:Ag = 1:1	−55~150 °C, 2 cycles/h, 450 cycles	48.54	40	[39]
Kato et al.	2017	**Cu** + **Sn-8 wt.% Cu**(<13 μm), content: Cu:Sn = 7:3	−40~250 °C, 1000 cycles	42	40	[49]
Gao et al.	2020	**Cu** particles, **Cu oxide** fragments, **Cu oxide**nanoparticles; Formic acid as reducing solvent	−40~200 °C, 1 cycles/h, 500 cycles	~27.5	~28	[53]
Wu et al.	2022	**Cu** (spherical particles 20–60 nm, 0.2–0.6 μm and 1–2 μm) + **MWCNTs** (content: 0.6 wt%)	−65~150 °C, 54 min/cycles, 225 cycles	26.64 MPa	23.91	[63]

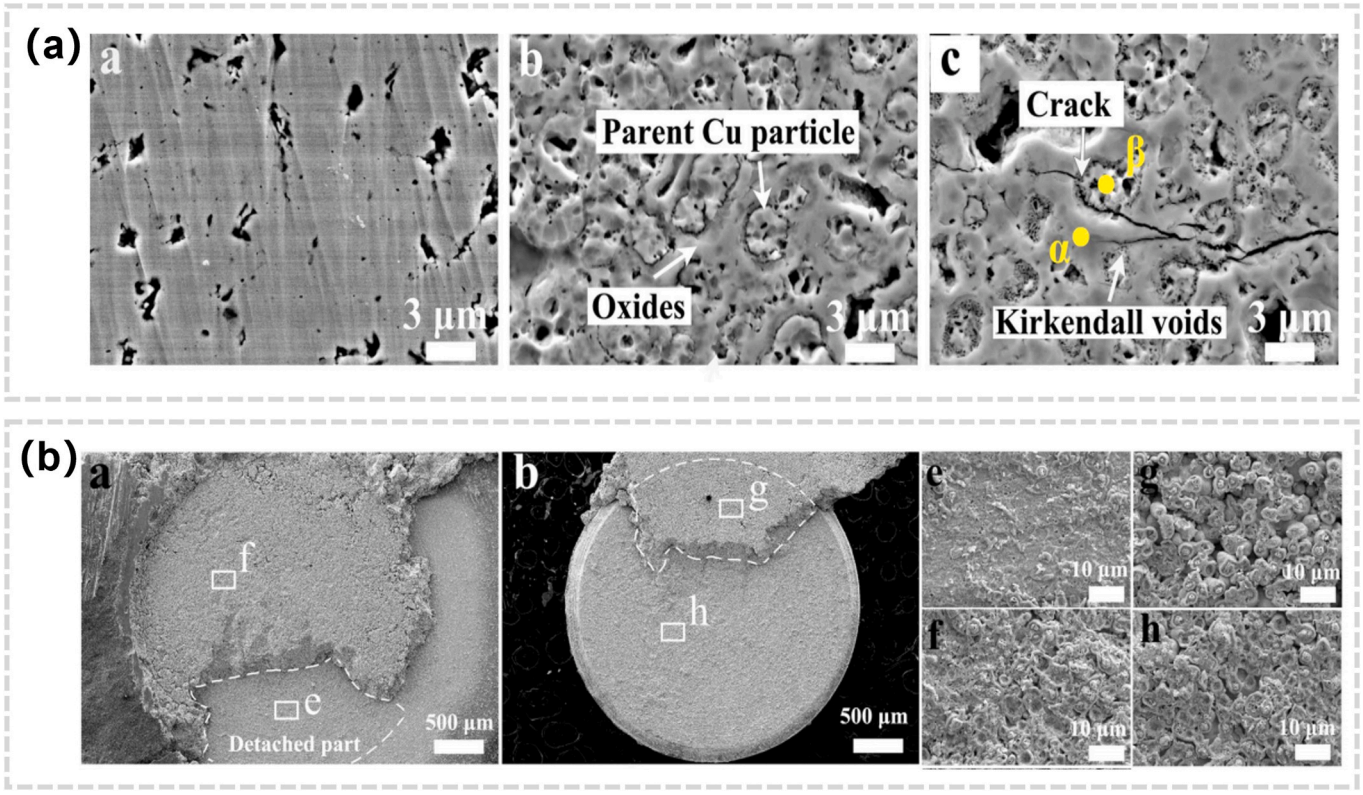

Fig. 16. (a)Cross-sectional SEM images of Cu–Cu bonding specimens after thermal cycling: as-sintered, 200 cycles, and 500 cycles [53];(b)Fracture surfaces of the bottom side and upper side of Cu–Cu bonding specimens after 500 thermal cycles [53].

materials, investigations into Cu-based composite sintered materials have so far been limited. Moreover, galvanic corrosion, which generally accelerates the degradation of composite sintered materials in harsh environments, presents an additional concern.

3.4. Electrochemical migration test

Electrochemical migration (ECM) is a common reliability issue in electronic materials, primarily caused by applied bias in the presence of an electrolyte. The growth of conductive dendrites can lead to short circuits and catastrophic failure in electronic devices. The ECM phenomenon was first observed in the late 1940s, with the increasing miniaturization of electronic products and their widespread usage, ECM has garnered growing attention from both academia and industry. This is due to the increasing reliability problems related to ECM in electronic products. Current ECM research primarily focuses on silver [114–116], Sn, and Sn alloys [33,117–119].

ECM occurs when a positive and negative voltage is applied to two closely spaced electrodes, which are connected by a continuous electrolyte layer. The presence of an electrolyte layer, which can be either visible or an invisible adsorption layer, is a prerequisite for ECM. The formation of the electrolyte layer is influenced by factors such as relative humidity, contaminants, temperature, and the surface conditions of materials in the electronic product. Humidity is a key factor; Lee et al. [120] reported that at room temperature and humidity levels of about 60 % to 70 %, several monolayers of water could form on the metal surface, initiating the electrochemical migration process. Once the conditions for forming an electrolytic cell are met, the anode metal electrode under forward bias loses electrons and gradually dissolves into the electrolyte in the form of metal ions. These metal ions migrate towards the cathode under the influence of the internal electric field, where they gain electrons and undergo a reduction reaction, resulting in metal deposition [121], as shown in Fig. 18a. Current tests on electrochemical migration mainly rely on optical microscopes and

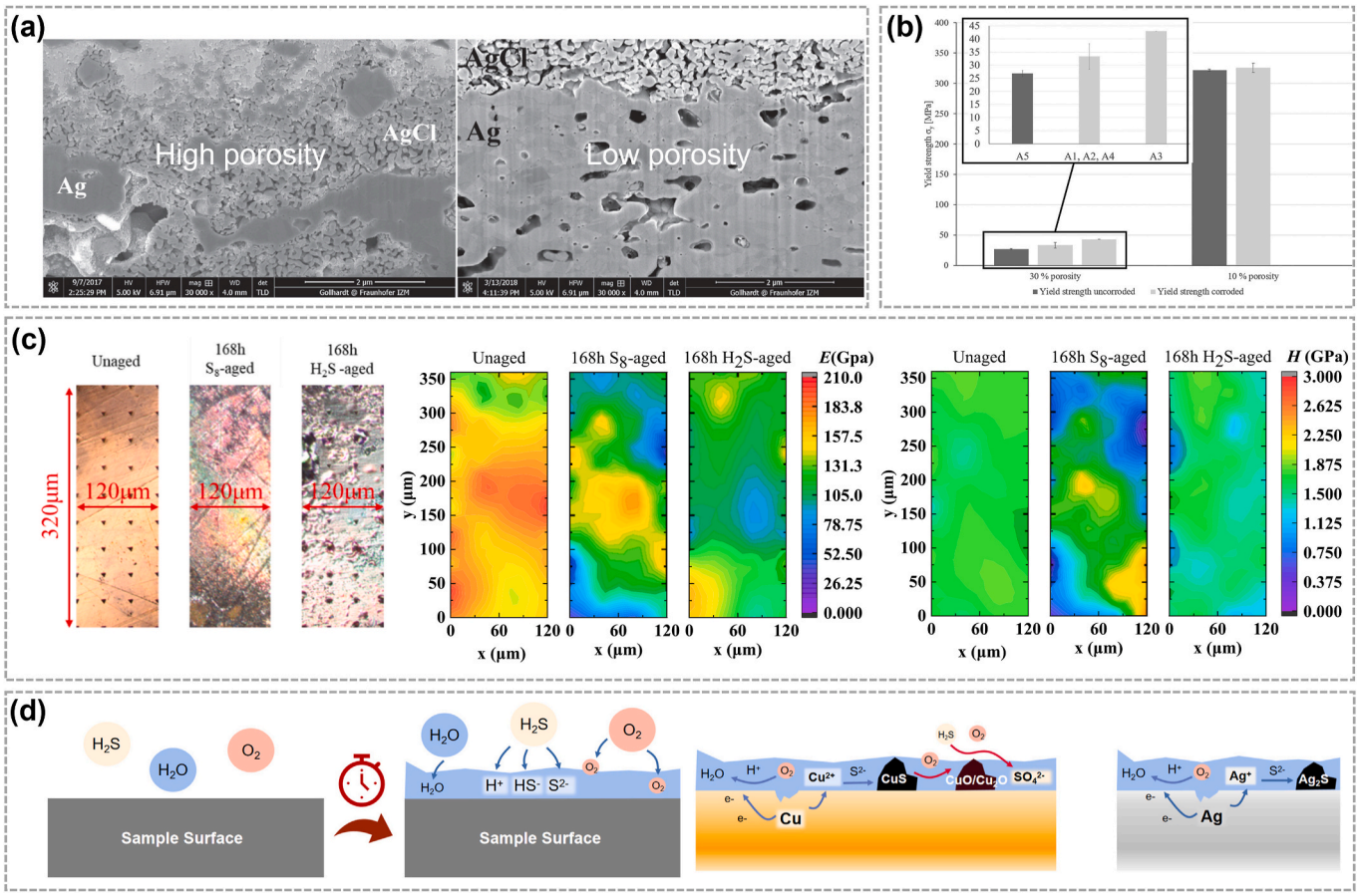

Fig. 17. Study on chemical and galvanic corrosion of chip interconnect materials: (a) FIB cross-section images of high-porosity and low-porosity sintered silver samples after corrosion [109].(b) Comparison of the yield strength of the uncorroded and corroded samples as a function of porosity [110].(c) The morphology of different nanoindentation test areas, and the elastic modulus (E) and hardness (H) distribution of each test area [113]. (d) Schematic diagram of the surface changes of copper and silver samples after corrosion and the mechanism by which copper oxide further inhibits copper corrosion [34].

electrochemical workstations, and their basic principles are shown in Fig. 18b [47].

The shape and morphology of the electrodeposit and the surface roughness largely depend on the current path and the concentration of substances involved in the electrolysis process [122]. Due to the uneven current distribution on the electrode surface, metal ions may preferentially nucleate and grow at specific locations on the cathode, resulting in dendrite formation. Dendrite formation occurs in two main stages: initiation and propagation. A critical overpotential is required for dendrite initiation, and studies have shown that most of the time is spent during this initiation stage rather than the propagation stage [123]. During propagation, dendrites with needle-like or tree-like shapes grow more rapidly at their tips compared to other parts of the electrode. This is due to several reasons: (1) As the dendrite grows, the distance between the dendrite tip and the anode decreases, creating a stronger electric field at the tip, which promotes further metal ion deposition. (2) The ion transport path to the dendrite tip is shorter than to other parts of the electrode, leading to preferential deposition at the tip. (3) As the dendrite tip sharpens, spherical diffusion replaces linear diffusion, increasing the deposition rate of metal ions at the tip.

In power devices, sintered silver chip interconnection materials are subject to challenges associated with electrochemical migration. Silver atoms can easily migrate under an electric field in humid or high-temperature environments, leading to short circuits and eventual device failure. Mixing a second phase with Ag nanoparticles has proven to be an effective method to enhance resistance to electrochemical migration. Research has shown that Cu exhibits superior electrochemical migration resistance, which has further promoted the study of sintered copper interconnect materials.

For instance, Ogura et al. [54] formulated a sintering paste containing a reducing solvent, silver oxide (Ag_2O), and copper oxide (CuO) to create a sintered joint. During the sintering process, Ag_2O was reduced to silver nanoparticles at 150 °C, while CuO was reduced to copper nanoparticles at approximately 300 °C. The study found that the resistance to electrochemical migration of this sintered joint was about four times greater than that of a pure sintered silver joint. Guo et al. [47] investigated the anti-electrochemical migration performance and mechanisms of mixed nanopastes comprising Ag nanoparticles, Ag nanowires, and Cu nanoparticles, as shown in Fig. 18c. The study showed that increasing the Cu nanoparticle content effectively prolonged the ECM time of the mixed nanopastes, as the Cu oxidation products ahead of the dendrites inhibited Ag migration. Consequently, Cu nanoparticles improved the resistance of the mixed nanopastes to electrochemical migration. Li et al. [124] prepared a Cu@Ag interconnect layer using electromagnetic compaction and examined its electrochemical migration behavior with a water drop test. The results indicated that the electrochemical migration resistance of Cu@Ag sinter joints exhibited better electrochemical migration resistance than nano-Ag sintered joints at a voltage of 5 V. Even when the voltage increased to 10 V, Cu@Ag joints failed only after 980 s, demonstrating superior performance (Fig. 18d). Cui et al. introduced a versatile complexation-based synthesis yielding Cu@Ag nanoparticles that outperform both pure Cu and Ag in resisting oxidation and ion migration under oxygenated conditions [125,126]. This also showed that the core-shell design of Cu@Ag gave it excellent anti-electrochemical migration performance.

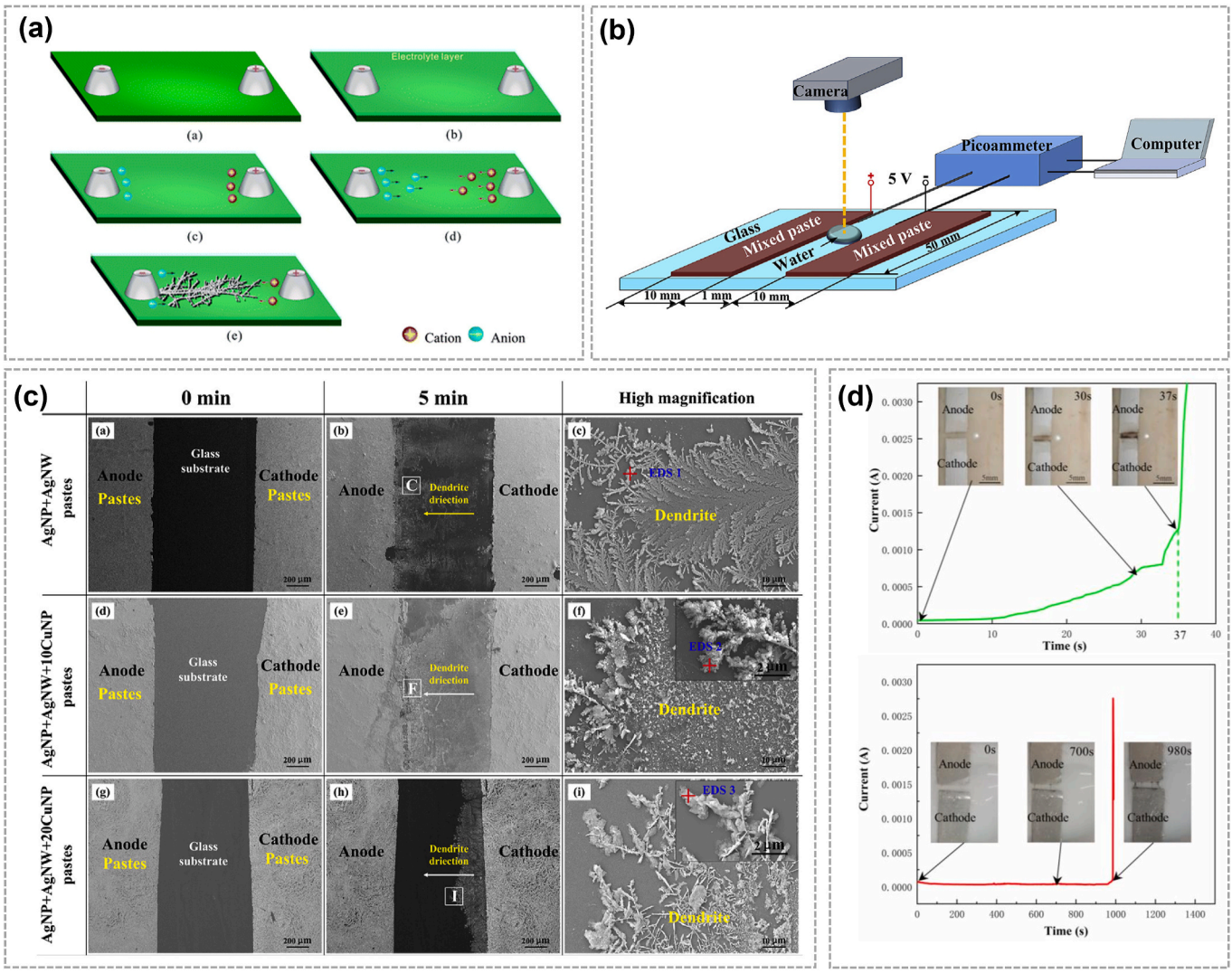

Fig. 18. Electrochemical Migration Principles and Testing Methods: (a) Schematic representation of the dendrite growth process [121]. (b) Diagram of the electrochemical migration test setup [47]. (c) Evaluation of electrochemical migration performance for various mixed nano-pastes [47]. (d) Comparison of electrochemical migration and short-circuit behavior between nanosilver and Cu@Ag interconnect materials [124].

Research on ECM in chip interconnect materials underscores significant reliability challenges in harsh environments, particularly for power devices exposed to high humidity and temperature. The growth of conductive dendrites can cause catastrophic device failure, highlighting the need for a deeper understanding of ECM mechanisms. Previous studies on ECM in silver, tin, and composite materials have provided a strong foundation for developing new Cu-based interconnect materials with enhanced resistance to electromigration.

4. Conclusion and prospects

Copper-based composite sintered materials present significant promise as reliable and cost-effective alternatives for die-attach applications in high-power electronics packaging. This review systematically analyzes recent progress in their development, emphasizing design strategies, material performance, and process optimization techniques. Three major enhancement approaches, including direct mixing, core–shell structuring, and alloying, are discussed, along with the influence of key sintering parameters such as temperature, pressure, and reducing atmosphere. The incorporation of diverse fillers (metallic, oxide, and non-metallic) and the use of advanced sintering techniques (e.g., TLPS, SPS, cold spray) have been shown to improve thermal, electrical, and mechanical properties of Cu-based composites. In addition, critical challenges such as oxidation resistance, long-term reliability, and industrial scalability are carefully examined. In summary, each of the three main strategies for enhancing Cu-based sintered materials offers distinct advantages and faces specific challenges. To facilitate clearer comparison and guide material selection in practical applications, a comparative summary of their key properties and process trade-offs is presented in Table 7. As seen from the table, direct mixing allows simple processing and tunable properties via filler selection, but often suffers from limited oxidation resistance. Core-shell structures offer better stability and lower sintering temperatures, though at higher material and synthesis costs. Alloying strategies provide a balance between performance and scalability, particularly in high-temperature applications, but may involve more complex sintering behavior. This comparative analysis provides a foundation for assessing material selection based on packaging reliability demands.

Despite substantial progress, several key challenges remain to be addressed for the widespread adoption and long-term reliability of Cu-based sintered materials:

(1) **Oxidation and Stability Issues:** Oxidation during sintering and service life remains a major limitation, as the formation of Cu_2O

Table 7
Comparative analysis of enhancement strategies for Cu-based sintered materials.

Strategy	Sintering Temp. (°C)	Shear Strength (MPa)	Oxidation Resistance	Process Complexity	Industrial Compatibility
Direct mixing	250~380	10~50	Low	Low	High
Core–shell structure	200~300	20~60	High	Medium	Moderate
Alloying	180~300	20~50	Medium to High	High	Medium

and CuO impedes particle coalescence and degrades bonding performance. The development of robust oxidation-resistant coatings (e.g., Cu@Sn, Cu@Ag) and the application of cost-effective, environmentally friendly reducing agents (such as ascorbic acid and glycerol) are promising directions for mitigating this issue. These approaches can help preserve surface activity and facilitate low-temperature sintering below 250 °C.

(2) **Long-Term Reliability under Harsh Environments:** Prolonged high-temperature exposure and thermal cycling often lead to interfacial degradation, void formation, and excessive intermetallic compound (IMC) growth. Incorporating functional nanofillers such as carbon nanotubes (CNTs) or epoxy-based reinforcements have shown potential to enhance interfacial strength (>30 MPa) and suppress defect evolution. Future efforts should focus on improving filler dispersion and understanding the reinforcement mechanisms under cyclic stress (>1000 cycles).

(3) **Process Optimization and Industrial Scalability:** Emerging sintering techniques such as spark plasma sintering (SPS), cold spray, and transient liquid phase sintering (TLPS) enable dense joint formation at reduced temperatures. However, industrial implementation remains limited by high equipment cost, energy demands, and limited throughput. To meet manufacturing scalability requirements, it is essential to develop simplified, energy-efficient sintering methods that ensure consistent bonding quality at temperatures below 250 °C while maintaining porosity levels under 5 % and shear strength above 25–30 MPa. Compatibility with various substrate types and geometric designs will also be vital for large-scale deployment.

(4) **Microstructure-Property Correlation:** A more quantitative understanding of how microstructural characteristics, such as grain size, IMC morphology, pore distribution, and interfacial quality, affect the thermal, electrical, and mechanical behavior of Cu-based joints is essential. For instance, maintaining thermal conductivity above 200 W/m·K and electrical conductivity over 80 % International Annealed Copper Standard (IACS, ~1.724 μΩ cm), requires precise control of densification and phase formation during sintering. The integration of advanced in-situ characterization techniques (e.g., transmission electron microscopy, synchrotron X-ray diffraction) and multiscale computational simulations will play a critical role in optimizing microstructure design and accelerating predictive material development.

In conclusion, copper-based composite sintered materials hold immense potential for next-generation high-power electronic packaging due to their cost-effectiveness, excellent mechanical stability, and electrical and thermal conductivity. Future advancements will rely on an interdisciplinary approach, integrating innovative material design, advanced processing techniques, and in-depth microstructural analysis. With continued research and development, Cu-based composites are poised to become a cornerstone for reliable, high-performance electronic devices operating under extreme conditions.

CRediT authorship contribution statement

Xinyue Wang: Writing – original draft, Investigation, Formal analysis, Data curation. **Zhoudong Yang:** Writing – original draft, Formal analysis, Data curation. **Letao Bian:** Writing – original draft, Formal analysis, Data curation. **Wenting Liu:** Visualization, Formal analysis, Data curation. **Guoqi Zhang:** Writing – review & editing, Supervision, Conceptualization. **Jing Zhang:** Writing – review & editing, Supervision. **Chuantong Chen:** Supervision, Writing – review & editing. **Pan Liu:** Writing – review & editing, Supervision, Funding acquisition, Conceptualization.

Consent for publication

The authors declare that this manuscript has not been published previously and is not under consideration for publication elsewhere.

Declaration of competing interest

The authors declare that they have no known competing financial interests or personal relationships that could have appeared to influence the work reported in this paper.

Acknowledgments

In this work, the authors would like to thank the National Natural Science Foundation of China under Grant 62304051, Shanghai Science & Technology Commission under Grant 24500790700, Shanghai SiC Power Devices Engineering & Technology Research Center (19DZ2253400), and Heraeus Materials Technology Shanghai Ltd. for funding this research. Many thanks to Chat Generative Pre-Trained Transformer (ChatGPT, OpenAI) for language help.

References

[1] B. Shi, A.I. Ramones, Y. Liu, H. Wang, Y. Li, S. Pischinger, J. Andert, A review of silicon carbide MOSFETs in electrified vehicles: application, challenges, and future development, IET Power Electron. 16 (12) (2023) 2103–2120, https://doi.org/10.1049/pel2.12524.

[2] Y. Mei, P. Ning, G. Lei, Z. Zeng, Editorial for the special issue on high reliability power device packaging and assistant technology in EV application, Journal of Power Supply 22 (3) (2024) 15–21, https://doi.org/10.13234/j.issn.2095-2805.2024.3.15.

[3] S.L. Zhao, Y. Tong, C.B. Wang, E.R. Yao, Challenges and progress in packaging materials for power modules with high operation temperature: review, J. Mater. Sci. Mater. Electron. 35 (35) (2024) 30, https://doi.org/10.1007/s10854-024-14002-4.

[4] W. Liu, X. Wang, J. Zhang, G. Zhang, P. Liu, Al-clad Cu bond wires for power electronics packaging: microstructure evolution, mechanical performance, and molecular dynamics simulation of diffusion behaviors, Mater. Today Commun. 41 (2024), https://doi.org/10.1016/j.mtcomm.2024.110940.

[5] R. Khazaka, L. Mendizabal, D. Henry, Review on joint shear strength of nano-silver paste and its long-term high temperature reliability, J. Electron. Mater. 43 (7) (2014) 2459–2466, https://doi.org/10.1007/s11664-014-3202-6.

[6] H. Zhang, J. Minter, N.-C. Lee, A brief review on high-temperature, Pb-free die-attach materials, J. Electron. Mater. 48 (1) (2018) 201–210, https://doi.org/10.1007/s11664-018-6707-6.

[7] A.J. Bell, O. Deubzer, Lead-free piezoelectrics—the environmental and regulatory issues, MRS Bull. 43 (8) (2018) 581–587, https://doi.org/10.1557/mrs.2018.154.

[8] L.J. T, G.C. M, D. B, J. G, D.W. Bergman, Examining the environmental impact of lead-free soldering alternatives, IEEE Trans. Electron. Packag. Manuf. 24 (1) (2002) 4–9, https://doi.org/10.1109/6104.924786.

[9] A. Kroupa, D. Andersson, N. Hoo, J. Pearce, A. Watson, A. Dinsdale, S. Mucklejohn, Current problems and possible solutions in high-temperature lead-free soldering, J. Mater. Eng. Perform. 21 (5) (2012) 629–637, https://doi.org/10.1007/s11665-012-0125-3.

[10] X. Lu, L. Zhang, W. Xi, M.-l. Li, Structure and properties of low-Ag SAC solders for electronic packaging, J. Mater. Sci. Mater. Electron. 33 (29) (2022) 22668–22705, https://doi.org/10.1007/s10854-022-09091-y.

[11] S.A. Paknejad, S.H. Mannan, Review of silver nanoparticle based die attach materials for high power/temperature applications, Microelectron. Reliab. 70 (2017) 1–11, https://doi.org/10.1016/j.microrel.2017.01.010.
[12] X. Wang, Z. Zeng, G. Zhang, J. Zhang, P. Liu, Joint analysis and reliability test of epoxy-based nano silver paste under different pressure-less sintering processes, J. Electron. Packag. 144 (4) (2022), https://doi.org/10.1115/1.4053432.
[13] P. Zhang, X. Jiang, P. Yuan, H. Yan, D. Yang, Silver nanopaste: synthesis, reinforcements and application, Int. J. Heat Mass Tran. 127 (2018) 1048–1069, https://doi.org/10.1016/j.ijheatmasstransfer.2018.06.083.
[14] C. Du, G. Zou, Z. A, B. Lu, B. Feng, J. Huo, Y. Xiao, Y. Jiang, L. Liu, Highly accurate and efficient prediction of effective thermal conductivity of sintered silver based on deep learning method, Int. J. Heat Mass Tran. 201 (2023), https://doi.org/10.1016/j.ijheatmasstransfer.2022.123654.
[15] Z. Cui, Q. Jia, H.Q. Zhang, Y.S. Wang, L.M. Ma, G.S. Zou, F. Guo, Review on shear strength and reliability of nanoparticle sintered joints for power electronics packaging, J. Electron. Mater. 53 (6) (2024) 2703–2726, https://doi.org/10.1007/s11664-024-10970-9.
[16] T.F. Chen, K.S. Siow, Comparing the mechanical and thermal-electrical properties of sintered copper (Cu) and sintered silver (Ag) joints, J. Alloys Compd. 866 (2021), https://doi.org/10.1016/j.jallcom.2021.158783.
[17] W. Liu, J. Wang, Y. Gao, L. Ji, J. Zhang, G. Zhang, P. Liu, Simulation, prediction and verification of the thermal and electrical properties of sintered copper joints with random pore structure for power electronics packaging, 2024 25th International Conference on Electronic Packaging Technology (ICEPT), 2024, pp. 1–6, doi: 10.1109/ICEPT63120.2024.10668544.
[18] Y.J. Wang, D. Xu, H.D. Yan, C.F. Li, C.T. Chen, W.L. Li, Low-temperature copper sinter-joining technology for power electronics packaging: a review, J. Mater. Process. Technol. 332 (2024) 25, https://doi.org/10.1016/j.jmatprotec.2024.118526.
[19] L.M. Ma, Z.Y. Lu, Q. Jia, Y.S. Wang, H.Q. Zhang, W. Zhou, G.S. Zou, F. Guo, Research progress of Cu nanoparticle sintering technology for power electronic packaging, Rare Met. Mater. Eng. 53 (1) (2024) 296–320, https://doi.org/10.12442/j.issn.1002-185X.20230170.
[20] M. Nishimoto, R. Tokura, M.T. Nguyen, T. Yonezawa, Copper materials for low temperature sintering, Mater. Trans. 63 (5) (2022) 663–675, https://doi.org/10.2320/matertrans.MT-N2021004.
[21] F.P. McCluskey, H. Greve, Thermal conductivity of Cu-Sn transient liquid phase sintered interconnects for high power density modules, Delft, Netherlands (2017), https://doi.org/10.1109/IWIPP.2017.7936768.
[22] K. Li, Y. Liu, J. Zhang, N. Xiao, A low cost multi-shapes designed sintering composite paste: A strengthening method of sintered interconnect for die attach in high temperature applications, Mater. Lett. 315 (2022), https://doi.org/10.1016/j.matlet.2022.131884.
[23] C. Chen, S. Zhao, T. Sekiguchi, K. Suganuma, Large-scale bare Cu bonding by 10 μm-sized Cu–Ag composite paste in low temperature low pressure air conditions, J. Sci. Adv. Mater. Devices 8 (3) (2023), https://doi.org/10.1016/j.jsamd.2023.100606.
[24] B.-U. Hwang, K.-H. Jung, K.D. Min, C.-J. Lee, S.-B. Jung, Pressureless Cu–Cu bonding using hybrid Cu–epoxy paste and its reliability, J. Mater. Sci. Mater. Electron. 32 (3) (2021) 3054–3065, https://doi.org/10.1007/s10854-020-05055-2.
[25] R. Gao, S. He, Y.-A. Shen, H. Nishikawa, Effect of substrates on fracture mechanism and process optimization of oxidation–reduction bonding with copper microparticles, J. Electron. Mater. 48 (4) (2019) 2263–2271, https://doi.org/10.1007/s11664-019-07046-4.
[26] H. Ji, J. Zhou, M. Liang, H. Lu, M. Li, Ultra-low temperature sintering of Cu@Ag core-shell nanoparticle paste by ultrasonic in air for high-temperature power device packaging, Ultrason. Sonochem. 41 (2018) 375–381, https://doi.org/10.1016/j.ultsonch.2017.10.003.
[27] J. Wang, L. Zhang, F. Duan, F. Wang, W. Zhang, K. Xu, H. Chunjin, H. Chen, Transient liquid phase bonding of Cu@Sn core–shell particles with added Sn–3.0Cu–0.5Ag, J. Mater. Sci. 57 (12) (2022) 6640–6655, https://doi.org/10.1007/s10853-022-07013-1.
[28] H. Yang, Study on the preparation process and sintering performance of doped nano-silver paste, Rev. Adv. Mater. Sci. 61 (1) (2022) 969–976, https://doi.org/10.1515/rams-2022-0273.
[29] J. Liu, W. Lv, C. Chen, Y. Kang, Atomic insight in fusion mechanism of heterogeneous and homogeneous sintering: Cu and Ag nanoparticles, Results Phys. 57 (2024), https://doi.org/10.1016/j.rinp.2024.107411.
[30] W. Liu, X. Wang, J. Zhang, G. Zhang, C. Chen, P. Liu, Quartet structure generation set algorithm based 3D reconstruction on porous structures of sintered copper joints for power electronics packaging, Scr. Mater. 265 (2025), https://doi.org/10.1016/j.scriptamat.2025.116750.
[31] H. Shao, A. Wu, Y. Bao, Y. Zhao, G. Zou, L. Liu, Novel transient liquid phase bonding through capillary action for high-temperature power devices packaging, Mater. Sci. Eng., A 724 (2018) 231–238, https://doi.org/10.1016/j.msea.2018.03.097.
[32] X. Chen, P. Liu, P. Liu, H. Chen, Preparation of copper-graphene layered composites by spark plasma sintering, Mater. Sci. Technol. 34 (14) (2018) 1693–1699, https://doi.org/10.1080/02670836.2018.1472908.
[33] D. Minzari, M.S. Jellesen, P. Møller, R. Ambat, On the electrochemical migration mechanism of tin in electronics, Corros. Sci. 53 (10) (2011) 3366–3379, https://doi.org/10.1016/j.corsci.2011.06.015.
[34] X. Wang, Z. Yang, B. Wang, W. Chen, G. Zhang, J. Zhang, J. Fan, P. Liu, Effect of epoxy resin addition on properties and corrosion behavior of sintered joints in power modules serviced offshore, J. Mater. Res. Technol. 25 (2023) 6593–6612, https://doi.org/10.1016/j.jmrt.2023.07.098.
[35] F. Hou, Z. Sun, M. Su, J. Fan, X. You, J. Li, Q. Wang, L. Cao, G. Zhang, Review of die-attach materials for SiC high-temperature packaging, IEEE Trans. Power Electron. 39 (10) (2024) 13471–13486, https://doi.org/10.1109/tpel.2024.3417529.
[36] T. Kim Seah, C. Kuan Yew, Physical and electrical characteristics of silver-copper nanopaste as alternative die-attach, IEEE Trans. Compon. Packag. Manuf. Technol. 4 (1) (2014) 8–15, https://doi.org/10.1109/tcpmt.2013.2285128.
[37] A. Kawecki, T. Knych, E. Sieja-Smaga, A. Mamala, P. Kwaśniewski, G. Kiesiewicz, B. Smyrak, A. Pacewicz, Fabrication, properties and microstructures of high strength and high conductivity copper-silver wires/otrzymywanie oraz Własności I Mikrostruktura Wysokowytrzymałych I Wysoko Przewodzących Drutów Ze Stopów Cu-Ag, Arch. Metall. Mater. 57 (4) (2012) 1261–1270, https://doi.org/10.2478/v10172-012-0141-1.
[38] Y.-T. Cheng, K.-L. Lin, C.-C. Lin, Preparing Silver–Copper pastes in accordance with percolation theory for die attach bonding, Mater. Chem. Phys. 297 (2023), https://doi.org/10.1016/j.matchemphys.2023.127391.
[39] X. Wang, H. Chen, Z. Yang, W. Liu, Z. Zeng, G. Zhang, J. Zhang, J. Fan, P. Liu, Microstructure evolution and micromechanical behavior of solvent-modified Cu–Ag composite sintered joints for power electronics packaging at high temperatures, J. Mater. Res. Technol. 30 (2024) 8433–8450, https://doi.org/10.1016/j.jmrt.2024.05.196.
[40] W. Lv, J. Liu, Y. Mou, Y. Ding, M. Chen, F. Zhu, Fabrication and sintering behavior of nano Cu–Ag composite paste for high-power device, IEEE Trans. Electron. Dev. 70 (6) (2023) 3202–3207, https://doi.org/10.1109/ted.2023.3268252.
[41] F. Lang, H. Yamaguchi, H. Nakagawa, H. Sato, Thermally stable bonding of SiC devices with ceramic substrates: transient liquid phase sintering using Cu/Sn powders, J. Electrochem. Soc. 160 (8) (2013) D315–D319, https://doi.org/10.1149/2.114308jes.
[42] G. Yang, W. Lin, H. Lai, C. Zhong, Y. Zhang, C. Cui, Improved understanding of the enhancement of sintering of mixtures of Cu microparticles and sn nanoparticles for electronic packaging, J. Mater. Sci. Mater. Electron. 33 (14) (2022) 11467–11474, https://doi.org/10.1007/s10854-022-08119-7.
[43] M.Z. Siah, D.C. Yborde, N.L. Sukiman, S. Ramesh, Y.H. Wong, Effects of resin binder on characteristics of sintered aluminum–copper nanopaste as high-temperature die-attach material, IEEE Trans. Compon. Packag. Manuf. Technol. 9 (10) (2019) 2104–2110, https://doi.org/10.1109/tcpmt.2019.2912176.
[44] K.D. Min, K.-H. Jung, C.-J. Lee, B.-U. Hwang, S.-B. Jung, Enhancement of electrochemical and thermal bonding reliability by forming a Cu3Sn intermetallic compound using Cu and Sn–58Bi, J. Alloys Compd. 857 (2021), https://doi.org/10.1016/j.jallcom.2020.157595.
[45] S.A.M. Hannes Greve, F. Patrick McCluskey, Reliability of paste based transient liquid phase sintered interconnects. 2014 Electronic Components & Technology Conference, IEEE, Orlando, FL, USA, 2014, https://doi.org/10.1109/ECTC.2014.6897462.
[46] J. Li, X. Yu, T. Shi, C. Cheng, J. Fan, S. Cheng, T. Li, G. Liao, Z. Tang, Depressing of Cu Cu bonding temperature by composting Cu nanoparticle paste with Ag nanoparticles, J. Alloys Compd. 709 (2017) 700–707, https://doi.org/10.1016/j.jallcom.2017.03.220.
[47] W. Guo, H. Zhang, X. Zhang, L. Liu, P. Peng, G. Zou, Y.N. Zhou, Preparation of nanoparticle and nanowire mixed pastes and their low temperature sintering, J. Alloys Compd. 690 (2017) 86–94, https://doi.org/10.1016/j.jallcom.2016.08.060.
[48] Y. Liu, Z. Li, H. Zhang, F. Sun, Microstructure and mechanical properties of nano-Ag sintered joint enhanced by Cu foam, J. Mater. Sci. Mater. Electron. 30 (16) (2019) 15795–15801, https://doi.org/10.1007/s10854-019-01965-y.
[49] F. K, F. L, H. N, H. Y, R. K, K. Okada, Thermal resistance evaluation of die-attachment made of nano-composite Cu/Sn TLPS paste in SiC power module, 2017 International Conference on Electronics Packaging (ICEP), 2017 Yamagata, Japan, doi: 10.1109/ECTC.2014.6897439.
[50] R. Mohd Said, M.A.A. Mohd Salleh, N. Saud, M.I.I. Ramli, H. Yasuda, K. Nogita, Microstructure and growth kinetic study in Sn–Cu transient liquid phase sintering solder paste, J. Mater. Sci. Mater. Electron. 31 (14) (2020) 11077–11094, https://doi.org/10.1007/s10854-020-03657-4.
[51] X. Liu, H. Nishikawa, Low-pressure Cu-Cu bonding using in-situ surface-modified microscale Cu particles for power device packaging, Scr. Mater. 120 (2016) 80–84, https://doi.org/10.1016/j.scriptamat.2016.04.018.
[52] D. Yamagiwa, T. Matsuda, H. Furusawa, K. Sato, H. Tatsumi, T. Sano, Y. Kashiba, A. Hirose, Pressureless sinter joining of bare Cu substrates under forming gas atmosphere by surface-oxidized submicron Cu particles, J. Mater. Sci. Mater. Electron. 32 (14) (2021) 19031–19041, https://doi.org/10.1007/s10854-021-06418-z.
[53] R. Gao, S. He, J. Li, Y.-A. Shen, H. Nishikawa, Interfacial transformation of preoxidized Cu microparticles in a formic-acid atmosphere for pressureless Cu–Cu bonding, J. Mater. Sci. Mater. Electron. 31 (17) (2020) 14635–14644, https://doi.org/10.1007/s10854-020-04026-x.
[54] T. Ogura, T. Yagishita, S. Takata, T. Fujimoto, A. Hirose, Bondability of copper joints formed using a mixed paste of Ag_2O and CuO for low-temperature sinter bonding, Mater. Trans. 54 (6) (2013) 860–865, https://doi.org/10.2320/matertrans.MD201202.
[55] B.J. Han, J.-H. Lee, Compressive sinter bonding in air between Cu finishes using paste containing composite Ag2O-Cu filler, Electron. Mater. Lett. 19 (6) (2023) 543–553, https://doi.org/10.1007/s13391-023-00430-7.

[56] T. Yao, T. Matsuda, T. Sano, C. Morikawa, A. Ohbuchi, H. Yashiro, A. Hirose, In situ study of reduction process of CuO paste and its effect on bondability of Cu-to-Cu joints, J. Electron. Mater. 47 (4) (2018) 2193–2197, https://doi.org/10.1007/s11664-017-6049-9.
[57] J. Hou, Q. Zhang, S. He, J. Bian, J. Jiu, C. Li, H. Nishikawa, Large-area and low-cost Cu–Cu bonding with cold spray deposition, oxidation, and reduction processes under low-temperature conditions, J. Mater. Sci. Mater. Electron. 32 (15) (2021) 20461–20473, https://doi.org/10.1007/s10854-021-06556-4.
[58] R.U.S.W. Park, S. Nagao, T. Sugahara, Y. Katoh, H. Ishino, K. Sugiura, K. Tsuruta, K. Suganuma. Low-pressure sintering bonding with Cu and CuO flake paste for power devices, IEEE, Orlando, FL, USA, 2014, https://doi.org/10.1109/ECTC.2014.6897439.
[59] T. Matsuda, S. Yamada, S. Okubo, A. Hirose, Antioxidative copper sinter bonding under thermal aging utilizing reduction of cuprous oxide nanoparticles by polyethylene glycol, J. Mater. Sci. 58 (40) (2023) 15617–15633, https://doi.org/10.1007/s10853-023-08976-5.
[60] Y. Zuo, S. Carter-Searjeant, M. Green, L. Mills, S.H. Mannan, Low temperature Cu joining by in situ reduction-sintering of CuO nanoparticle for high power electronics, Adv. Powder Technol. 31 (10) (2020) 4135–4144, https://doi.org/10.1016/j.apt.2020.08.019.
[61] Y. Gao, W. Li, C. Chen, H. Zhang, J. Jiu, C.-F. Li, S. Nagao, K. Suganuma, Novel copper particle paste with self-reduction and self-protection characteristics for die attachment of power semiconductor under a nitrogen atmosphere, Mater. Des. 160 (2018) 1265–1272, https://doi.org/10.1016/j.matdes.2018.11.003.
[62] R. Vignesh Babu, S. Kanagaraj, Sintering behaviour of Copper/carbon nanotube composites and their characterization, Adv. Powder Technol. 30 (10) (2019) 2200–2210, https://doi.org/10.1016/j.apt.2019.06.035.
[63] L. Wu, J. Qian, F. Zhang, J. Yu, Z. Wang, H. Guo, X. Chen, Low-temperature sintering of Cu/functionalized multi-walled carbon nanotubes composite paste for power electronic packaging, IEEE Trans. Power Electron. (2021), https://doi.org/10.1109/tpel.2021.3103563, 1-1.
[64] M.Gutierrez, N. Wang, M. K. Samani, L. Ye, J. Liu, Sintering of SiC enhanced copper paste for high power applications, 2017 IMAPS Nordic Conference on Microelectronics Packaging (NordPac), 2017, doi:10.1109/NORDPAC.2017.7993183.
[65] G. Yang, Q. Zhang, Q. Fang, W. Li, H. Wei, T. Zhao, Y. Zhang, G. Huang, C. Cui, K. Zhang, Preparation of nickel nanoparticle-decorated graphene/copper composites with enhanced interfacial bonding and heat dissipation properties, J. Alloys Compd. 1028 (2025), https://doi.org/10.1016/j.jallcom.2025.180696.
[66] J.Y. Kim, J.A. Rodriguez, J.C. Hanson, A.I. Frenkel, P.L. Lee, Reduction of CuO and Cu2O with H2: H embedding and kinetic effects in the formation of suboxides, J. Am. Chem. Soc. 125 (35) (2003) 10684–10692, https://doi.org/10.1021/ja0301673.
[67] N. Ozawa, M. Shibata, Reduction process of copper oxide film by formic acid, Jpn. J. Appl. Phys. 60 (11) (2021), https://doi.org/10.35848/1347-4065/ac28e0.
[68] S. Deng, X. Zhang, G.D. Xiao, K. Zhang, X. He, S. Xin, X. Liu, A. Zhong, Y. Chai, Thermal interface material with graphene enhanced sintered copper for high temperature power electronics, Nanotechnology 32 (31) (2021), https://doi.org/10.1088/1361-6528/abfc71.
[69] X. Wang, Z. Yang, L. Ji, Z. Zeng, H. Chen, J. Fan, P. Liu, An SEM-based finite element analysis of Cu-Ag sintered joints on thermal shock reliability, 2024 25th International Conference on Electronic Packaging Technology (ICEPT), 2024 Tianjin, China, doi: 10.1109/ICEPT63120.2024.10668475.
[70] M. Park, B.-H. Kim, S. Kim, D.-S. Han, G. Kim, K.-R. Lee, Improved binding between copper and carbon nanotubes in a composite using oxygen-containing functional groups, Carbon 49 (3) (2011) 811–818, https://doi.org/10.1016/j.carbon.2010.10.019.
[71] H. Wei, Z. Zhang, Z. Li, L. Peng, G. Yang, T. Zhao, Y. Zhang, G. Huang, C. Cui, Silver/graphene oxide composite with high thermal/electrical conductivity and mechanical performance developed through a dual-dispersion medium method, J. Mater. Res. Technol. 33 (2024) 8211–8221, https://doi.org/10.1016/j.jmrt.2024.11.163.
[72] Y. Wang, D. Xu, H. Yan, C.-F. Li, C. Chen, W. Li, Low-temperature copper sinter-joining technology for power electronics packaging: a review, J. Mater. Process. Technol. 332 (2024), https://doi.org/10.1016/j.jmatprotec.2024.118526.
[73] S.-J. Oh, T.G. Kim, S.-Y. Kim, Y. Jo, S.S. Lee, K. Kim, B.-H. Ryu, J.-U. Park, Y. Choi, S. Jeong, Newly designed Cu/Cu10Sn3 core/shell nanoparticles for liquid phase-photonic sintered copper electrodes: large-area, low-cost transparent flexible electronics, Chem. Mater. 28 (13) (2016) 4714–4723, https://doi.org/10.1021/acs.chemmater.6b01709.
[74] L. Wang, F. Xia, W. Xu, G. Wang, S. Hong, F. Cheng, B. Wu, N. Zheng, Antioxidant high-conductivity copper pastes based on core–shell copper nanoparticles for flexible printed electronics, Adv. Funct. Mater. 33 (26) (2023), https://doi.org/10.1002/adfm.202215127.
[75] Z. Li, C. Yu, Y. Wen, Y. Gao, X. Xing, Z. Wei, H. Sun, Y.-W. Zhang, W. Song, Mesoporous hollow Cu–Ni alloy nanocage from core–shell Cu@Ni nanocube for efficient hydrogen evolution reaction, ACS Catal. 9 (6) (2019) 5084–5095, https://doi.org/10.1021/acscatal.8b04814.
[76] E.B. Choi, J.-H. Lee, Submicron Ag-coated Cu particles and characterization methods to evaluate their quality, J. Alloys Compd. 689 (2016) 952–958, https://doi.org/10.1016/j.jallcom.2016.08.009.
[77] S. Shang, A. Kunwar, Y. Wang, X. Qi, H. Ma, Y. Wang, Synthesis of Cu@Ag core–shell nanoparticles for characterization of thermal stability and electric resistivity, Appl. Phys. A 124 (7) (2018), https://doi.org/10.1007/s00339-018-1887-8.
[78] W. Cao, W. Li, R. Yin, W. Zhou, Controlled fabrication of Cu–Sn core–shell nanoparticles via displacement reaction, Colloids Surf. A Physicochem. Eng. Asp. 453 (2014) 37–43, https://doi.org/10.1016/j.colsurfa.2014.03.088.
[79] H. Chen, T. Hu, M. Li, Z. Zhao, Cu@Sn core–shell structure powder preform for high-temperature applications based on transient liquid phase bonding, IEEE Trans. Power Electron. 32 (1) (2017) 441–451, https://doi.org/10.1109/tpel.2016.2535365.
[80] T. Hu, H. Chen, M. Li, C. Wang, Microstructure evolution and thermostability of bondline based on Cu@Sn core-shell structured microparticles under high-temperature conditions, Mater. Des. 131 (2017) 196–203, https://doi.org/10.1016/j.matdes.2017.06.022.
[81] J.H. Bae, J.M. Cha, B.K. Ryu, Production of Cu@SiO(2) core-shell nanoparticles with antibacterial properties, J. Nanosci. Nanotechnol. 19 (3) (2019) 1690–1694, https://doi.org/10.1166/jnn.2019.16152.
[82] T. Yamauchi, Y. Tsukahara, T. Sakata, H. Mori, T. Yanagida, T. Kawai, Y. Wada, Magnetic Cu-Ni (core-shell) nanoparticles in a one-pot reaction under microwave irradiation, Nanoscale 2 (4) (2010) 515–523, https://doi.org/10.1039/b9nr00302a.
[83] A. Farid, A.S. Khan, M. Javid, M. Usman, I.A. Khan, A.U. Ahmad, Z. Fan, A. A. Khan, L. Pan, Construction of a binder-free non-enzymatic glucose sensor based on Cu@Ni core-shell nanoparticles anchored on 3D chiral carbon nanocoils-nickel foam hierarchical scaffold, J. Colloid Interface Sci. 624 (2022) 320–337, https://doi.org/10.1016/j.jcis.2022.05.137.
[84] K.-L. Wu, Y.-M. Cai, B.-B. Jiang, W.-C. Cheong, X.-W. Wei, W. Wang, N. Yu, Cu@Ni core–shell nanoparticles/reduced graphene oxide nanocomposites for nonenzymatic glucose sensor, RSC Adv. 7 (34) (2017) 21128–21135, https://doi.org/10.1039/c7ra00910k.
[85] D.-E. Lee, S. Moru, R. Bhosale, W.-K. Jo, S. Tonda, Cu–Ni core–shell bimetallic cocatalyst decorated polymeric carbon nitride for highly efficient and selective methane production from photocatalytic CO2 reduction, Appl. Surf. Sci. 599 (2022), https://doi.org/10.1016/j.apsusc.2022.153973.
[86] T. Hu, H. Chen, M. Li, Die attach materials with high remelting temperatures created by bonding Cu@Sn microparticles at lower temperatures, Mater. Des. 108 (2016) 383–390, https://doi.org/10.1016/j.matdes.2016.06.099.
[87] Q. Dong, C. Huang, G. Duan, F. Zhang, D.a. Yang, Facile synthesis and electrical performance of silica-coated copper powder for copper electronic pastes on low temperature co-fired ceramic, Mater. Lett. 186 (2017) 263–266, https://doi.org/10.1016/j.matlet.2016.09.116.
[88] T.G. Kim, H.J. Park, K. Woo, S. Jeong, Y. Choi, S.Y. Lee, Enhanced oxidation-resistant Cu@Ni core-shell nanoparticles for printed flexible electrodes, ACS Appl. Mater. Interfaces 10 (1) (2018) 1059–1066, https://doi.org/10.1021/acsami.7b14572.
[89] E.B. Choi, Y.-J. Lee, J.-H. Lee, Rapid sintering by thermo-compression in air using a paste containing bimodal-sized silver-coated copper particles and effects of particle size and surface finish type, J. Alloys Compd. 897 (2022), https://doi.org/10.1016/j.jallcom.2021.163223.
[90] X. Wang, Z. Zeng, J. Zhang, G. Zhang, P. Liu, Simulation and verification or Cu@Ag core-shell sintered paste for power semiconductor die-attach applications, 2022 IEEE 72nd Electronic Components and Technology Conference (ECTC), 2022, pp. 507–512, doi: 10.1109/ECTC51906.2022.00086.
[91] H. Chen, X. Wang, Z. Zeng, G. Zhang, J. Zhang, P. Liu, Solvent modulation, microstructure evaluation, process optimization, and nanoindentation analysis of micro-Cu@Ag core–shell sintering paste for power electronics packaging, J. Mater. Sci. Mater. Electron. 34 (24) (2023), https://doi.org/10.1007/s10854-023-11083-5.
[92] Q. Gao, W. Zhou, Z. Xia, X. Wang, Y. Wang, Z. Yue, F. Guo, Investigation of ethylene glycol, α-terpineol, and polyethylene glycol 400 on the sintering properties of Cu–Ag core–shell micro/nano-mixed paste, J. Mater. Sci. Mater. Electron. 34 (21) (2023), https://doi.org/10.1007/s10854-023-10965-y.
[93] K. Wang, J. Wen, J. Feng, Y. Wang, P. Wu, S. Wang, Y. Tian, A novel Cu@Ag nano paste with low porosity for rapidly sintering in air condition, Mater. Char. 209 (2024), https://doi.org/10.1016/j.matchar.2024.113762.
[94] Y. Kim, J.-H. Lee, Suppression of Ag dewetting in submicron Cu@Ag particles in paste for improving sinter bondability through surface modification, J. Mater. Res. Technol. 30 (2024) 3558–3570, https://doi.org/10.1016/j.jmrt.2024.04.118.
[95] J. Liu, H. Liu, F. Yu, X. Wang, J. Wang, C. Hang, H. Chen, M. Li, Cu@Sn@Ag core–shell particles preform for power device packaging under harsh environments, J. Mater. Sci. Mater. Electron. 32 (11) (2021) 14703–14714, https://doi.org/10.1007/s10854-021-06026-x.
[96] X. Mao, J. Liu, F. Yu, X. Fu, C. Hang, H. Chen, M. Li, A high-temperature-resistant die attach material based on Cu@In@Ag particles for high-power devices, J. Mater. Sci. Mater. Electron. 33 (8) (2022) 5599–5612, https://doi.org/10.1007/s10854-022-07747-3.
[97] Y. Zhang, X. Yu, Z. Chen, S. Wu, H. Lai, S. Ta, T. Lin, G. Yang, C. Cui, Synthesis of imidazole-compound-coated copper nanoparticles with promising antioxidant and sintering properties, Micromachines (Basel) 14 (11) (2023), https://doi.org/10.3390/mi14112079.
[98] Y. Zhang, Q. Liu, Y. Liu, J. Tong, Z. Huang, S. Wu, P. Liang, G. Yang, C. Cui, Green synthesis of novelin situmicro/submicron-Cu paste for semiconductor interconnection, Nanotechnology 33 (28) (2022), https://doi.org/10.1088/1361-6528/ac4b79.
[99] J.-W. Yoon, S. Bae, B.-S. Lee, S.-B. Jung, Bonding of power device to ceramic substrate using Sn-coated Cu micro paste for high-temperature applications, Appl. Surf. Sci. 515 (2020), https://doi.org/10.1016/j.apsusc.2020.146060.

[100] J.-W. Park, Y.-R. Jang, H.-S. Shin, H.-S. Kim, J.J. Kim, A study on copper/silver core–shell microparticles with silver nanoparticles hybrid paste and its intense pulsed light sintering characteristics for high oxidation resistance, International Journal of Precision Engineering and Manufacturing-Green Technology 8 (6) (2020) 1649–1661, https://doi.org/10.1007/s40684-020-00271-x.
[101] M. Won, D. Kim, H. Yang, C. Oh, Low-temperature sinterable Cu@Ag paste with superior strength driven by pre-heating process, Energies 16 (14) (2023), https://doi.org/10.3390/en16145419.
[102] B. Z, Q. J, Y. W, D. L, H. Z, H. H, L. M, G. Z, F. Guo, Preparation of Ag-Cu nanoparticle film using a dual-beam pulsed laser deposition for power electronic packaging, J. Laser Appl. (2024), https://doi.org/10.2351/7.0001321, 022010 (2024).
[103] D. Zhang, G. Zou, L. Liu, Y. Zhang, C. Yu, H. Bai, N. Zhou, Synthesis with glucose reduction method and low temperature sintering of Ag-Cu alloy nanoparticle pastes for electronic packaging, Mater. Trans. 56 (8) (2015) 1252–1256, https://doi.org/10.2320/matertrans.MI201406.
[104] J. Liu, Y. Mou, Y. Peng, Q. Sun, M. Chen, Novel Cu-Ag composite nanoparticle paste for low temperature bonding, Mater. Lett. 248 (2019) 78–81, https://doi.org/10.1016/j.matlet.2019.03.133.
[105] J. Yan, D. Zhang, G. Zou, L. Liu, Y.N. Zhou, Preparation of oxidation-resistant Ag-Cu alloy nanoparticles by polyol method for electronic packaging, J. Electron. Mater. 48 (2) (2018) 1286–1293, https://doi.org/10.1007/s11664-018-6771-y.
[106] R. Robinson, V. Krause, S. Wang, S. Yan, G. Shang, J. Gordon, S. Tycko, C. J. Zhong, Silver-copper alloy nanoinks for ambient temperature sintering, Langmuir 38 (18) (2022) 5633–5644, https://doi.org/10.1021/acs.langmuir.2c00221.
[107] L. Guo, W. Liu, X. Ji, Y. Zhong, C. Hang, C. Wang, Robust Cu–Cu bonding with multiscale coralloid nano-Cu3Sn paste for high-power electronics packaging, ACS Appl. Electron. Mater. 4 (7) (2022) 3457–3469, https://doi.org/10.1021/acsaelm.2c00376.
[108] E. Castillo, A.F. Pasha, Z.I. Larson, N. Dimitrov, New generation copper-based interconnection from nanoporous CuSn alloy film sintered at low temperatures, Mater. Adv. 5 (6) (2024) 2285–2295, https://doi.org/10.1039/d3ma01071f.
[109] E. Kolbinger, S. Wagner, A. Gollhardt, O. Rämer, K.D. Lang, Corrosion behaviour of sintered silver under maritime environmental conditions, Microelectron. Reliab. 88–90 (2018) 715–720, https://doi.org/10.1016/j.microrel.2018.07.123.
[110] E. Kolbinger, S. Kuttler, S. Wagner, M. Schneider-Ramelow, Investigation of the mechanical properties of corroded sintered silver layers by using Nanoindentation, Microelectron. Reliab. 114 (2020), https://doi.org/10.1016/j.microrel.2020.113889.
[111] J.I. A.-T, S.K. B, G. W, G. E, H.R. Kotadia, Understanding Cu sintering and its role on corrosion behaviour for high-temperature microelectronic application, 2023 24th European Microelectronics and Packaging Conference & Exhibition (EMPC), 2023 Cambridge, United Kingdom, doi: 10.23919/EMPC55870.2023.10418365.
[112] X. Wang, Z. Yang, G. Zhang, J. Zhang, P. Liu, Simulation, prediction, and verification of the corrosion behavior of Cu-Ag composite sintered paste for power semiconductor die-attach applications, 2023 IEEE 73rd Electronic Components and Technology Conference (ECTC), 2023, pp. 1982–1988, doi: 10.1109/ECTC51909.2023.00341.
[113] W. Chen, X. Liu, Z. Yang, D. Hu, X. Liu, X. Zhu, X. Fan, G. Zhang, J. Fan, Insights into sulfur and hydrogen sulfide induced corrosion of sintered nanocopper paste: a combined experimental and ab initio study, Mater. Des. 240 (2024), https://doi.org/10.1016/j.matdes.2024.112876.
[114] Y. Xu, Y. Liu, Z. Pan, K. Li, J. Lu, Q. Sun, Evaluating electrochemical migration behavior of sintered nano-Ag: factors of bias voltage, electrode spacing, sinter process parameters, and NaCl concentration, J. Mater. Sci. Mater. Electron. 34 (28) (2023), https://doi.org/10.1007/s10854-023-11369-8.
[115] Z. Ding, Z. Wang, B. Zhang, G.-Q. Lu, Y.-H. Mei, A reliable way to improve electrochemical migration (ECM) resistance of nanosilver paste as a bonding material, Appl. Sci. 12 (9) (2022), https://doi.org/10.3390/app12094748.
[116] S. Wan, H. Wang, J.-H. Liu, B.-K. Liao, X.-P. Guo, Self-assembled monolayers for electrochemical migration protection of low-temperature sintered nano-Ag paste, Rare Met. 41 (4) (2021) 1239–1244, https://doi.org/10.1007/s12598-021-01866-2.
[117] B. Liao, Z. Chen, Y. Qiu, G. Zhang, X. Guo, Effect of citrate ions on the electrochemical migration of tin in thin electrolyte layer containing chloride ions, Corros. Sci. 112 (2016) 393–401, https://doi.org/10.1016/j.corsci.2016.08.003.
[118] V. Verdingovas, M.S. Jellesen, R. Ambat, Effect of pulsed voltage on electrochemical migration of tin in electronics, J. Mater. Sci. Mater. Electron. 26 (10) (2015) 7997–8007, https://doi.org/10.1007/s10854-015-3454-9.
[119] D. Minzari, F.B. Grumsen, M.S. Jellesen, P. Møller, R. Ambat, Electrochemical migration of tin in electronics and microstructure of the dendrites, Corros. Sci. 53 (5) (2011) 1659–1669, https://doi.org/10.1016/j.corsci.2011.01.009.
[120] S. Lee, R.W. Staehle, Adsorption studies of water on copper, nickel, and iron using the quartz-crystal microbalance technique: assessment of BET and FHH models of adsorption, Mater. Corros. 48 (2) (2004) 86–94, https://doi.org/10.1002/maco.19970480203.
[121] X. Zhong, L. Chen, B. Medgyes, Z. Zhang, S. Gao, L. Jakab, Electrochemical migration of Sn and Sn solder alloys: a review, RSC Adv. 7 (45) (2017) 28186–28206, https://doi.org/10.1039/c7ra04368f.
[122] M. Sun, H.G. Liao, K. Niu, H. Zheng, Structural and morphological evolution of lead dendrites during electrochemical migration, Sci. Rep. 3 (2013) 3227, https://doi.org/10.1038/srep03227.
[123] X. Zhong, G. Zhang, Y. Qiu, Z. Chen, X. Guo, Electrochemical migration of tin in thin electrolyte layer containing chloride ions, Corros. Sci. 74 (2013) 71–82, https://doi.org/10.1016/j.corsci.2013.04.015.
[124] Z. Li, W. Zhao, R. Shi, Z. Chen, Z. Chen, L. Liu, Electrochemical migration mechanism of Cu@Ag composite preforms by electromagnetic compaction for power electronics, 2023 24th International Conference on Electronic Packaging Technology (ICEPT), 2023, pp. 1–4, doi: 10.1109/ICEPT59018.2023.10491934.
[125] G. Yang, Q. Zou, P. Wang, H. Lai, T. Lai, X. Zeng, Z. Li, J. Luo, Y. Zhang, C. Cui, Towards understanding the facile synthesis of well-covered Cu-Ag core-shell nanoparticles from a complexing model, J. Alloys Compd. 874 (2021), https://doi.org/10.1016/j.jallcom.2021.159900.
[126] G. Yang, P. Wang, Y. Liu, S. Lu, B. Luo, T. Lai, S. Ta, T. Lin, J. Luo, Y. Zhang, C. Cui, Effect of Ag coating on the oxidation resistance, sintering properties, and migration resistance of Cu particles, J. Alloys Compd. 923 (2022), https://doi.org/10.1016/j.jallcom.2022.166271.